Simulation Modelling of Stand-alone Triple Basin Solar Desalination System

A DISSERTATION

SUBMITTED IN PARTIAL FULFILLMENT OF THE REQUIREMENTS FOR THE AWARD OF THE DEGREE

OF

MASTER OF TECHNOLOGY

IN

THERMAL ENGINEERING

Submitted by

RAHUL KUMAR MEENA

(ROLL NO. 2K18/THE/09)

Under the supervision of

DR. PUSPENDRA SINGH

&

DR. ANIL KUMAR



DEPARTMENT OF MECHANICAL ENGIEERING DELHI TECHNOLOGICAL UNIVERSITY

(formerly Delhi College of Engineering)

Bawana Road, Delhi – 110042

May, 2022

DELHI TECHNOLOGICAL UNIVERSITY

(Formerly Delhi College of Engineering)

Bawana Road, Delhi – 110 042

CANDIDATE'S DECLARATION

I, Rahul Kumar Meena, Roll No. 2K18/THE/09 student of M.Tech (Thermal Engineering),

hereby declare that the project dissertation titled "Simulation Modelling of Stand-alone

Triple Basin Solar Desalination System" which is submitted by me to the Department of

Mechanical Engineering, Delhi Technological University, Delhi in partial fulfillment of the

requirement for the award of the degree of Master of Technology, is original and not copied

from any source without proper citation. This work has not previously formed the basis for

the award of any degree, Diploma Associateship, fellowship or other similar title or

recognition.

Place: Delhi

RAHUL KUMAR MEENA

Date: 10/05/2022

2

DELHI TECHNOLOGICAL UNIVERSITY

(Formally Delhi College of Engineering)

Bawana Road, Delhi -110042

CERTIFICATE

This is to certify that Project Dissertation entitled "Simulation Modelling of Stand-alone

Triple Basin Solar Desalination System", which is submitted by Rahul Kumar Meena,

Roll No. 2K18/THE/09 Department of Mechanical Engineering, Delhi Technological

University, Delhi in partial fulfillment of the requirement for the award of degree of Master

of Technology is the record of the project work carried out by the student under our

supervision. To the best of our knowledge, this work has not been submitted in part or full

for any Degree or Diploma to this University or elsewhere.

DR. PUSHPENDRA SINGH

SUPERVISOR

DR. ANIL KUMAR

SUPERVISOR

Date: 10/05/2022

Place: New Delhi

3

ABSTRACT

This project titled as "Simulation Modelling of Stand-alone Triple Basin Solar Desalination System" aims to design and analyze a water distillation system that can produce clean water from a contaminated source, and the system should be relatively portable, inexpensive, and relies solely on renewable source solar energy.

Inspiration for this project comes from my native place Danalpur at Karauli district of Rajasthan, which is situated at the bank of the river Gambhir. There is a shortage of pure drinking water. Water in the river is contaminated by dissolved salts and concentration of Fluoride above safe permissible limits. Hence, I decided to design a energy efficient potable Desalination System that can treat the saline/contaminated water at minimum cost, efficient and at the same time run from a clean source of energy.

From the literature, it has come to notice that the triple basin solar desalination system with cover cooling is designed by Srithar [30]. Some improvements were suggested depending on multiple other resources from the literature. Geometry for the triple basin solar desalination system equipped with parabolic concentrator is modelled on COMSOL and ANSYS. Simulation analysis is carried out on ANSYS FLUENT v19.2 at the atmospheric conditions of the Delhi region at 28.7041° N, 77.1025° E coordinates. All the modes of heat transfer and evaporation & condensation phenomena are examined above climatic conditions. Therefore, the dimensions and

geometry of the fins are varied as cylindrical and triangular. The heat-absorbing material in the fins is tested by varying it with charcoal and river sand. Within the is analysis domain, simulation results of the designated systems were calculated and comparison is carried out. The simulation results found that peak temperature is higher at the edge of fin in triangular geometry (73.112oC) compared to cylindrical fins (66.09°C). The maximum temperature of air and water-vapour mixture inside the system is 351.5 K, and the minimum temperature is 304.25 K. Parabolic concentrator causes the maximum sunlight to concentrate on the surface of the glass casing and that trapped radiation increases the temperature of the system. Peak temperature of the system raises to 78.35 °C for the current system. The maximum water production rate in a TBSS is 16.78 kg m⁻² day-1 when the system is equipped with heat storage material, concentrator, cooling water arrangement, and proper insulation.

ACKNOWLEDGEMENT

I, Rahul Kumar Meena, take this momentous opportunity to express my heartfelt gratitude,

ineptness & regards to vulnerable and highly esteemed guide, Dr. Pushpendra Singh,

Associate Professor, and Dr. Anil Kumar, Associate Professor, Department of Mechanical

Engineering, Delhi Technological University for providing us an opportunity to present our

project on "Simulation Modelling of Stand-alone Triple Basin Solar Desalination

System".

I with full pleasure converge our heartiest thanks to Prof. Vipin, HOD, Department of

Mechanical Engineering, Delhi Technological University, for their invaluable advice and

wholehearted cooperation without which this project would not have seen the light of day.

I attribute heartiest thanks to all the faculty members of the Department of Mechanical

Engineering and friends for their valuable advice and encouragement.

RAHUL KUMAR MEENA M.TECH, 2K18/THE/09

Department of Mechanical Engineering,

Delhi Technological University

6

CONTENTS

Candidates Declaration		
Certificate		
Abstract		
Acknowledge		
Contents		
List of Tables	viii	
List of figures	ix	
List of Symbols, Abbreviations	xi	
CHAPTER 1 INTRODUCTION		
1.1 Thermal Desalination	8	
1.1.1 Crystallization	8	
1.1.2 Evaporation	9	
1.2 Membrane Desalination	9	
1.2.1 Reverse Osmosis	9	
1.2.2 Electro-dialysis	10	
1.2.3 Distillation	10	
1.3 Solar desalination	10	
1.3.1 Solar still	11	
CHAPTER 2 LITERATURE REVIEW	14	
CHAPTER 3 METHODOLOGY	25	
3.1 Governing Equations	25	
3.1.1 Energy Equations	26	
3.1.2 Continuity Equations	26	
3.1.3 Momentum Equations	26	
3.1.4 Volume Conservation Equations	27	

3.1.5 Mass Transfer Equations	27
3.1.6 Pressure Constraints	27
3.1.7 Heat Transfer Equations	28
3.1.8 Water Production	29
3.1.9 Solar Irradiance Equations	29
3.2 Computational Fluid Dynamics Model of Modelling	29
3.2.1 Geometry Creation	31
3.2.2 Meshing	33
3.2.3 Initial and boundary conditions	33
CHAPTER 4 RESULTS AND DISCUSSION	35
4.1 Simulation Results	35
4.1.1 Temperature Distribution	35
4.1.2 Temperature Distribution with Time	42
4.1.3 Water Volume Fraction	43
4.1.4 Pressure Variation	47
4.1.5 Velocity Distribution	49
4.1.6 Mass Flow	50
4.1.7 Static Enthalpy	51
4.1.8 Absorption Coefficient	52
4.1.9 Turbulence Kinetic Energy	53
4.1.10 Eddy Velocity	54
4.1.11 Solar Heat Flux	55
4.1.12 Water Production Rate	56
CHAPTER 5 CONCLUSION	58
REFERENCES	60

LIST OF TABLES

S.No.	Topic
1.1	Different deaths reported by water-borne diseases In India 2014-2018
1.2	Categories of Desalination Processes
3.1	Geometry and properties
3.2	Boundary conditions for the simulation process
4.1	Peak Temperature comparison for triangular and cylindrical fins

LIST OF FIGURES

S.No.	Content
1.1	Water distribution on the planet earth
1.2	Symbolic representation of most affected states
1.3	Water index of States of India
1.4	Water demand estimation by 2030
1.5	Energy distribution of sources of energy
1.6	Direct normal solar radiation distribution in Indian sub-continent
1.7	Indian states cumulative solar installed capacity
1.8	Solar still principle
3.1	Single slope solar basin
3.2	Triple basin solar desalination model
3.3	Triple basin solar desalination model with internal geometry
3.4	Unstructured mesh of triple basin system and concentrator
4.1	Temperature distribution inside the pipes and water surface
4.2	Iso-surface temperature distribution inside the pipes and water surface
4.3	Temperature distribution of 4 triangular fins geometry
4.4	Temperature distribution of 4 cylindrical fins geometry
4.5	Irradiation heat flux distribution of 4 triangular fins geometry
4.6	Irradiation heat flux distribution of 4 cylindrical fins geometry

4.7	Temperature distribution inside triple basin still Side View			
4.8	Temperature distribution inside pipe flow			
4.9	Temperature distribution over the surface of parabolic concentrator			
4.10	Temperature distribution over the surface of parabolic concentrator an			
	pipe flow: combined system			
4.11	Temperature variation concerning the time of TBSS.			
4.12	Water volume fraction contour inside the glass of TBSS			
4.13	Water volume fraction contour on the glass of TBSS.			
4.14	Water volume fraction concerning the time of TBSS still			
4.15	Vapour volume fraction contour on the glass of TBSS			
4.16	Vapour volume fraction concerning the time of TBSS still.			
4.17	Vapour volume fraction concerning the time of TBSS.			
4.18	Pressure volume rendering inside the TBSS still.			
4.19	Pressure variation concerning time inside TBSS			
4.20	Velocity volume rendering inside the TBSS still			
4.21	Mass flow contour inside the TBSS still			
4.22	Mass flow contour inside the TBSS still.			
4.23	Static enthalpy volume rendering inside the TBSS still.			
4.24	Absorption coefficient volume rendering inside the TBSS still.			
4.25	Turbulence kinetic energy rendering inside the TBSS still.			
4.26	Eddy viscosity volume rendering inside the TBSS still.			
4.27	Solar heat flux concerning time inside the TBSS still			
4.28	Water production rate concerning time inside the TBSS still with			
	parabolic collector			

LIST OF SYMBOLS

 $\overline{v_m}$ = Mass averaged velocity, ms⁻¹

 k_t = Turbulent thermal conductivity which is defined according to the turbulence model, w/mk

 $a_k = \text{Absorptivity, l/mol-cm}$

 S_E = Sum of the heat of chemical reaction and any other volumetric heat sources, J

 ρ_m = Density of mixture, kg-m³

 \overline{F} = Gravitational body force and external body forces, kg-ms⁻²

 μ_m = Molecular viscosity of the mixture, N.s-m⁻²

 r_G = Volume fraction of gas.

 r_L = Volume fraction of liquid.

 $h_p^{f^i}$ = Formation enthalpy of species i of phase p, J/mol

 $h_q^{f^j}$ = Formation enthalpy of species i of phase q, J/mol

 h_p^i = Enthalpy of species i of phase p, J/mol

 H_p = Total enthalpy of phase p, J/mol

Hq = Total enthalpy of phase q, J/mol

 $h_{r\omega}$ = Radiative heat transfer coefficient form water to the glass, W/m²°C

 h_{cw} = Convective heat transfer coefficient from water to the glass, W/m²°C.

 $h_{e\omega}$ = Evapourative heat transfer coefficient from water to the glass, W/m²°C.

 $\varepsilon_{\omega} = \text{Emissivity}$

 T_w = Temperature of the water, oK

 P_w = Partial saturated vapour pressure at the water temperature, Nm⁻²

Pg = Partial saturated vapour pressure at the gas temperature, Nm⁻²

 σ = Stephan Boltzman, W/m² °C

 \dot{m}_{ew} = Distillate output, kg/s

 h_{fg} = Latent heat of vapourization of water, J/kg.

 δ = Sun declination angle, degree

n =Day of the year, starting from 1st January

 ω = Hour angle, degree.

 I_g = Hourly global irradiance, Wm⁻²

 I_b = Hourly diffuse radiation, Wm⁻²

 I_d = Hourly diffuse radiation, Wm⁻²

 I_{bn} = Beam radiation on the surface normal to the direction of the sun rays, Wm⁻²

DSSS = Double slope solar still

TDS = Total dissolved solids, mg-l⁻¹

SSS = Single slope solar still

RE = Renewable energy

SE = Solar Energy

D = Desalination

CHAPTER 1

INTRODUCTION

Water is a fundamental need of all living creatures, including humans and animals, for their survival and livelihood. Access to clean drinking water forms a priority. Availability of water for sanitation, agricultural activities, production, and manufacturing, etc. forms a vital need for human being's sustainability and growth.

Availability of water for various utilities can turn troubles into potential – facilitating people with timely reaching to work and office, and contributing to enhanced health levels for children, adults, and families worldwide e.

Under the current scenario, 78.5 crore people $\frac{1}{9}$ th lacks reach to safe drinkable water and 200 crore people $\frac{1}{3}$ rd lacks access to a toilet. Nearly 10 lakh people lose their lives each year due to sanitation and hygiene-related diseases, which could be curtailed to certain limits with access to safe water or sanitation. Every 2 minutes, a person dies from a water-borne disease [1].

Access to water for cleaning and sanitation-related activities contributes to an improved level of health and helps to prevent the outspread of infectious diseases.

Lack of freshwater resources and degrading water quality for various utilities is a severe concern to mankind and other living creatures on this earth. The situation gets worsens day by day due to human activities and environmental impacts on the water bodies. The only solution left with us is to reuse the water available in any form by filtering it and purifying it to make potable water fit for consumption with environment-friendly resources and those available in abundance like solar energy.

Various water bodies such as groundwater, rivers, ponds, oceans, etc. have plenty of water covering almost 71 % of the earth's area. Out of that, more than 96.5% is there in oceans, but it's highly saline and not suitable for drinking purposes. Only < 1% of fresh water is available or used for drinking purposes [2].

Degrading the quality of water day by day due to human civilization and industrial wastes is a major problem for the modern world. Therefore, the reusability of the water and treatment of contaminated water is of vital importance for the current generation so that our future generation can get water at least for their basic needs.

Also, conventional sources of energy are reducing day by day due to excessive exploitation of these resources. Their replenishment rate is limited, and they also cause severe damage to the environment due to pollution and the Green House Effect. Sun is a source of energy for our solar system. [31] 18.5 TWy (Tera-watt years) is the total energy demand of the earth population in 2015. Solar energy availability at the plane of the earth is estimated as 23000 TWy. i.e. if we can extract 0.08% of solar energy, our energy needs can be fulfilled without emitting polluting elements. It has ample energy irradiating on the surface of the earth that if we can use it to treat water, it can fulfill both these needs at the same time.

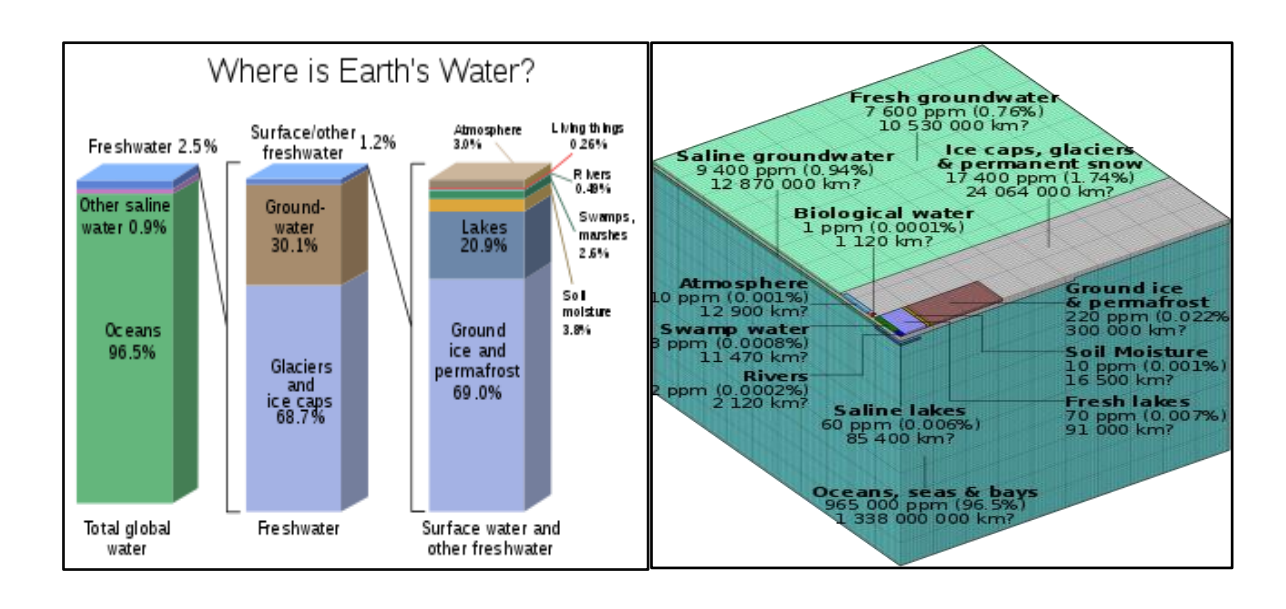
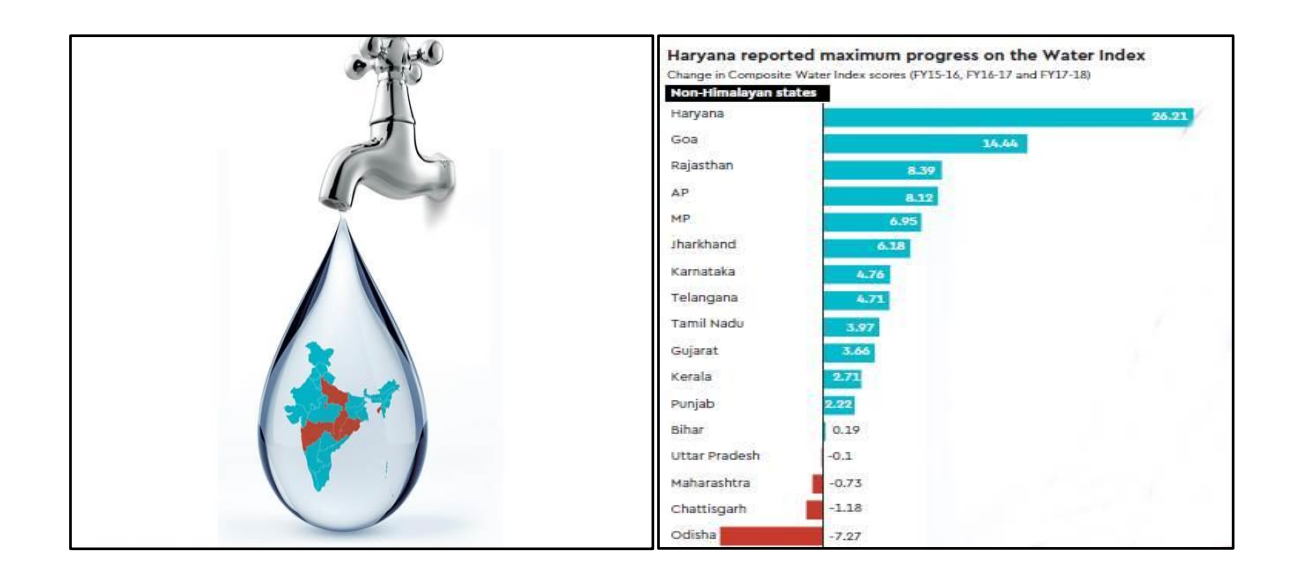


Fig 1.1 Water distribution on the planet earth [2]

The demand for water is increasing drastically day by day due to increased consumption and uncontrolled population growth. Indian population is 2nd highest in the world and by 2030 it will cross the population of China. With the increase in population, demand for resources will increase.

Fig 1.2 Symbolic representation of most effected states.

Fig 1.3 Water index of states of India.



Article published in Financial Express discussed the water crises in the Indian subcontinent, stating that the demand for water will exceed 2 times the supply of water by the year 2030. The average per capita water consumption in was 1654 cubic meters in 2016, which will reduce to 1341 cubic meters by 2025. By the year 2030, it will further reduce to 1140 cubic meters above the threshold limit of 1000 cubic meters. [Fig 4]. The industrial sector will also suffer due to this reduction in the availability of water. It will suffer a loss of 6% of the GDP of the state by the year 2050. [Fig 5]

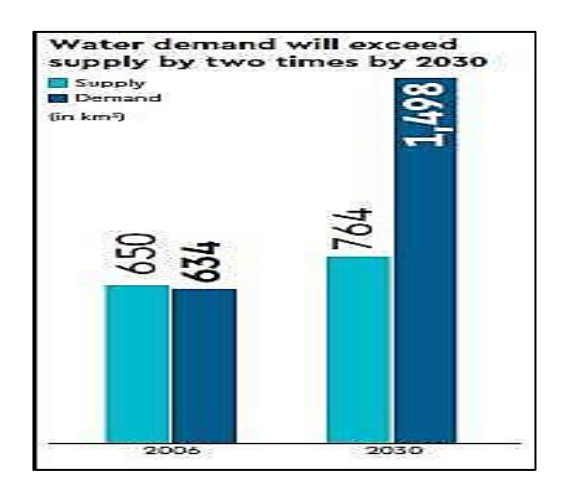


Fig 1.4 Water demand estimation by 2030

Due to the inadequate supply of fresh water and the inclusion of contaminants at some or the other stage, the health problem is regularly increasing. Globally, more than three billion people utilize drinkable water origin that is infected from excrement. Infected water can pass on infections such as polio, diarrhoea, dysentery, cholera, typhoid etc. According to the estimation, contaminated drinking water makes causes 485000 diarrhoeal deaths each year.

Table 1.1 Different deaths reported by water-borne diseases In India 2014-2018[3]

Water Borne Diseases claiming lives:					
Year	Cholera	ADD*	Typhoid	Viral Hepatitis	
2014	5	1337	425	400	
2015	4	1353	452	435	
2016	3	1555	511	451	
2017	3	1362	496	537	
2018	6	1450	399	584	
Total	21	7057	2283	2407	

^{*}Accute Diarrhoeal Diseases

Figure 6 shows the different cases and deaths reported by water-borne diseases in India from 2013 to 2017 while in 2018, more than 1.3 crore people were diagnosed with these water-borne diseases. And 2.2 million cases were reported in 2019. These cases are mostly reported in remote areas because necessary medical facilities are limited in remote areas [2]. Some common water-borne contaminants are carbonates, bicarbonates, and sulphates of calcium and magnesium, fluoride, nitrates, nitrites. In these contaminants, some are very harmful, which cause direct death, and other cause diseases.

Generally, heat is produced from conventional energy producers such as natural gases, oil, and coal. But these producers emit some harmful emissions such as carbon-di-oxide (CO_2), sulfur dioxide (SO_2), and nitrogen dioxide (NO_2). These emissions' effect on global warming may cause cancer and also can produce different harmful diseases. The researchers have realized these emissions may also cause of damaging the environment. Therefore, it needs more study on control of using conventional resources.

Distillation is one of the several processes used to treat water. This requires energy input in the form of heat, electricity or solar radiation. When solar energy is employed for this application, it is known as solar water distillation or solar desalination of brine.

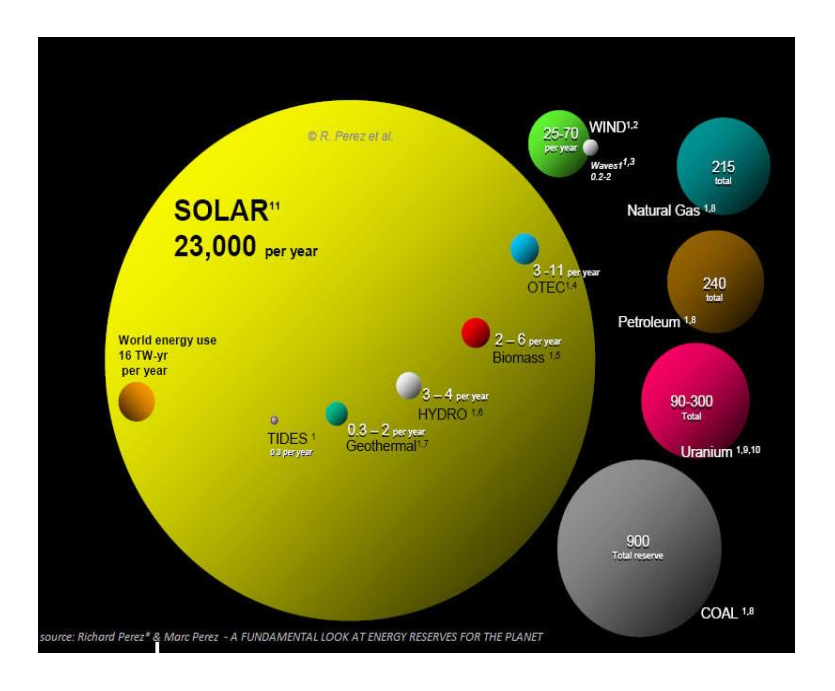


Fig 1.5 Energy distribution of sources of energy.

Solar desalination is a prominent process that results from the production of portable water free of cost using solar energy. This energy is used to evaporate water in a device commonly known "solar still". Solar stills are used in remote homes or during electrical evacuation in cases where well water, pipe or rainwater is not possible. Different versions are still used for spraying seawater, in desert survival kits, and for home water purification. For those who are unhappy with the quality of drinking water supplied by the municipality and the other purification methods are available to them, solar employed distillation or groundwater, tap water is a fun, efficient energy alternative. Solar distillation is a common option because of its simple technology, maintenance work and low energy consumption that does not require high-skill labour. India has a rich density for solar radiation throughout the states. The weather of India is such that it's dry and clear throughout the year. Thus, quality of radiation riches the surface. From the figure shown above, it is clear that the states near the tropic of cancer, western & middle part, the Ladakh region has immense potential for solar energy extraction. It was predicted that India will have

maximum solar irradiation globally with 2000kWh per square meter based on NASA projection.

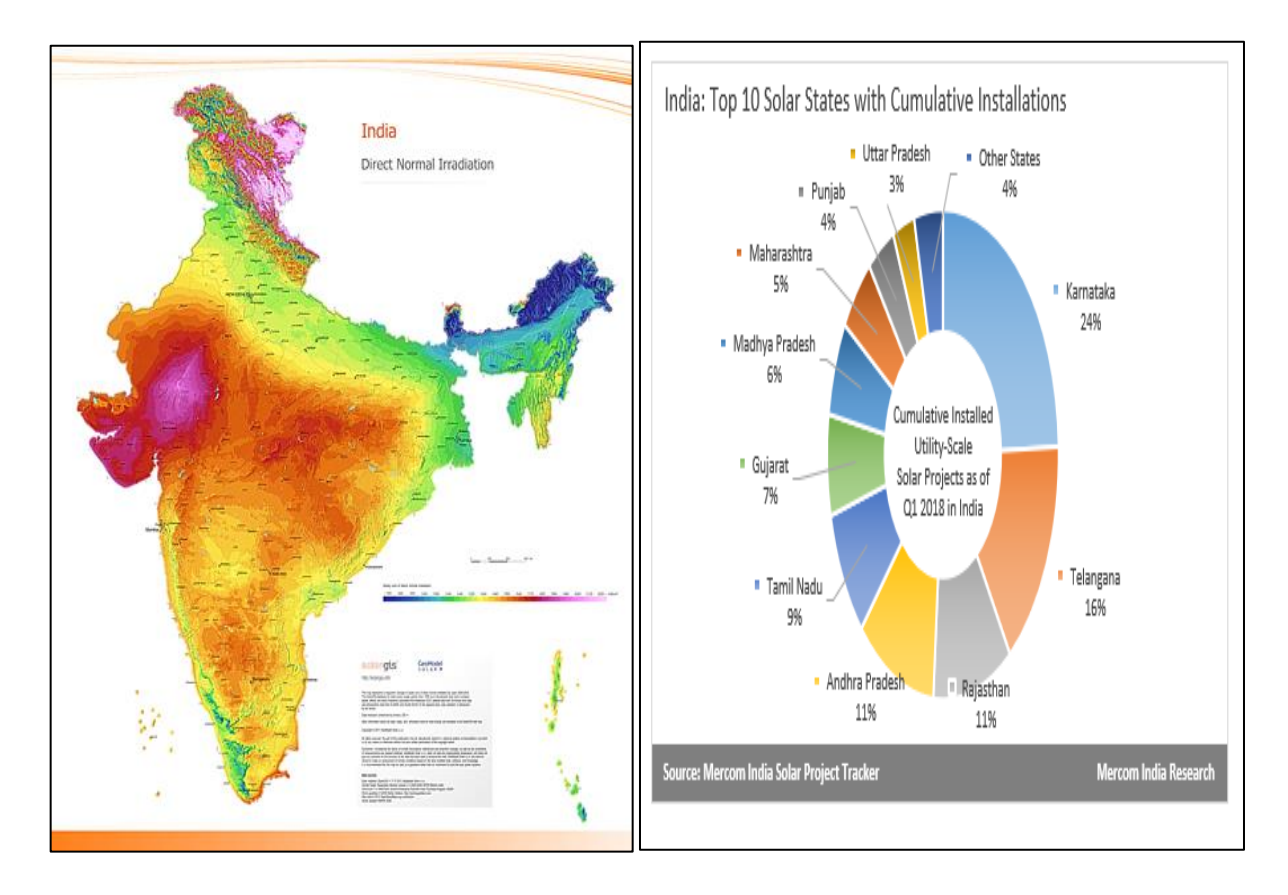


Fig 1.6 Direct Normal Solar radiation distribution in Indian Sub-continent [34]

Fig 1.7 Indian states Cumulative solar installed capacity.

Indian states like Telangana, Rajasthan, Andhra Pradesh, Gujrat etc. have lead in installing solar projects.

The energy emitted by the Sun is called solar energy. 23000TWy energy is available at the surface of earth, which is free. : The cost of extraction of this form of energy is costly at the present scenario, but technical advancement in this field will definitely reduce this cost drastically and make it a long-term solution for the energy requirements. Conventional sources are degrading and reducing at the great pace, and thus an alternative source needs the hour. Solar energy fulfils all our needs with environment concerns.

Water treatment from the available resources like groundwater, industrial and other wastewater, and saline water from the available purification techniques is the suitable way to fulfil the need of current and future generations for drinking, sanitation and industrial usage.

Classification of Different Water Purifications Techniques:

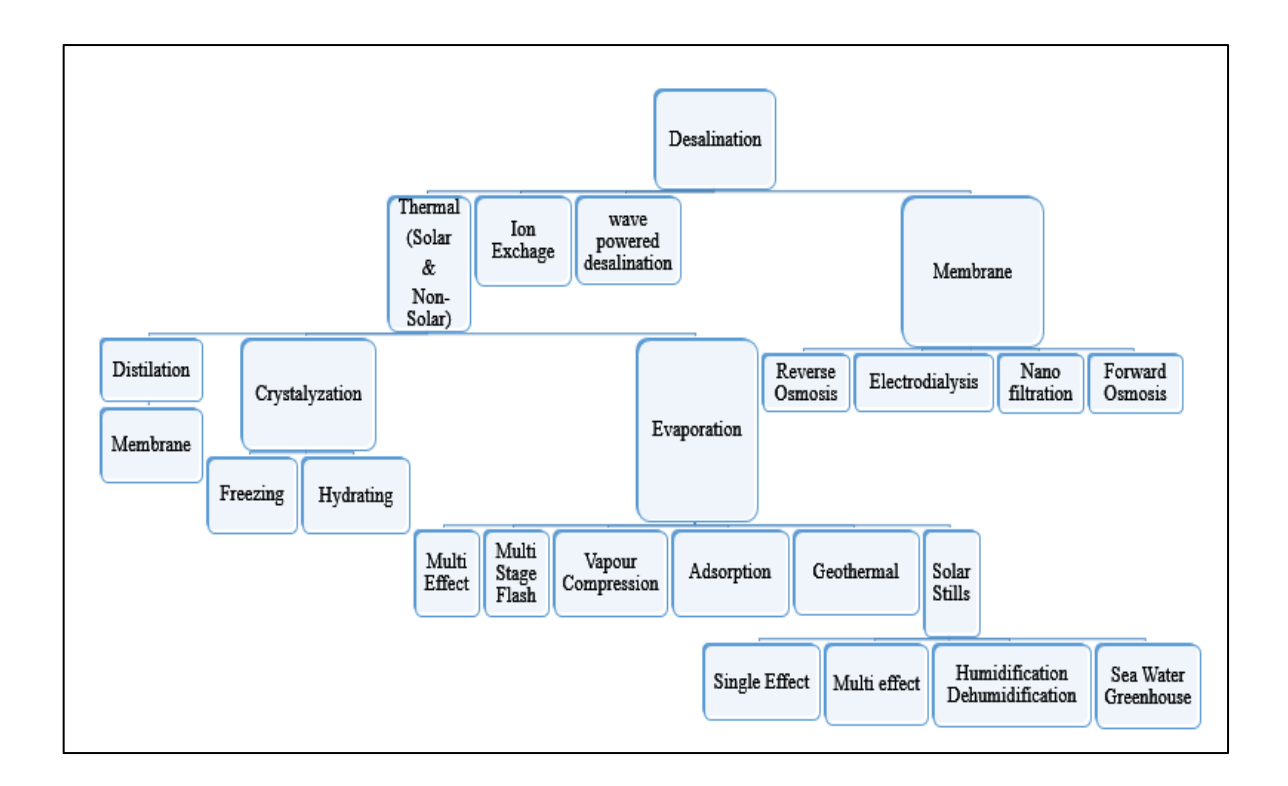
Single-phase process: Electro-dialysis, Reverse osmosis, Membrane distillation Multi-phase process: Flash desalination, Multi-effect distillation, Humidification dehumidification desalination, Vapour compression desalination, and solar still.

Solar energy is available in abundance, and a lot of research is already being carried out in this field to harness this form of clean and renewable energy.

1. Desalination Techniques:

Different apparatus are available to make the water potable to use. Also, researchers around a globe are trying to make the process more efficient and improve productivity so that it becomes a practical source to make the availability of water into the reach of common people.

Table 1.2: Categories of Desalination Processes [32]



1.1 Thermal Desalination:

It is the process where the heat energy is supplied to the system to pass it through the excited state and then, with due processes to desalinate the saline water. Heat energy can be supplied by conventional methods or from renewable sources of energy solar. Solar energy can be an ultimate source of energy and abundantly available free of cost. Thus, it can make the system cheap and efficient.

1.1.1 Crystallization:

It is a process in which a liquid's temperature is reduced at a slow rate to form its crystals.

1.1.1.1 Freezing Crystallization:

In this process, the solution is enriched by partly freezing it, and then the frozen material is separated from the liquid part left behind.

1.1.1.2 Hydrate distillation:

In this process, a solution is prepared so that the saline concentration of the saline water can be separated, which can easily be collected out.

1.1.2 Evaporation:

It is a process where the boiling point of mixture forms a means to separate them. Higher boiling liquids settled at the bottom and low boiling liquids change phase to vapour form and leave the solution collected.

1.1.3 Adsorption Desalination:

It is a process where a silica gel is used as a pair of adsorbent and de-adsorbent. It enhances the productivity of the desalination process by facilitating the process by increasing temperature difference by a considerable amount. Thus desalination stages can be increased with the inclusion of little amount of heat easily available by a renewable source of energy or industrial waste heat.

1.1.4 Multistage Flash Desalination:

In this process, the energy of the heated fluid is utilized in the next stage to heat the fluid of the next stage. This process is limited to 2-3 stages only. Thus a more efficient system as adsorption Desalination is preferred nowadays.

1.1.5 Multi-effect Desalination:

Process that separate's saline water by flashing a part of water into steam at multiple stages. These stages are countercurrent heat exchangers. This contributes to the production of portable water's 60% of the entire desalination process globally.

1.2 Membrane Desalination:

It is a process where a hydrophobic semi-permeable membrane acts as a hurdle for the liquid phase and allows the vapour form to penetrate through space.

1.2.1 Reverse Osmosis:

It is the reverse method of direct osmosis. It is the type of membrane desalination process. In this method, the external pressure is greater than osmatic pressure (pressure of more concentrated solution). Then the flow of pure water will be towards a less concentrated solution in the reverse direction. The result shows the globule is held on the higher forced side of the semi-porous diaphragm, and freshwater is obtained [7].

1.2.2 Electrodialysis (ED):

This method works based on how the charged particles move on the favorable side of electric flux. Positively charged particles are attracted by negatively charged particles and negative charge moves towards the positive charge outside the electro-dialysis cell. Still, in an electro-dialysis cell, cations can't cross the semi-permeable membrane. The consequence shows the globule is held with the membrane and pure water is obtained [7].

1.2.3 Distillation:

It is a process to separate components of a mixture due to their discrete boiling points.

1.3 Solar Desalination:

It is a process of desalinating the saline water with the help of solar energy available from the sun. Desalination process works on the principle of evaporative separation of dissolved salts from saline water. Further Treatment of distillate is necessary as some of the dissolved salts were there even after initial desalination due to evaporative separation. Apparatus employed for the same is called as Solar Still. A solar still is a device that converts the impure/saline water into distilled water by using solar energy in a small enclosed basin that involves simple condensation of vapours and low capital investment is needed for a potable system. However, this system lacks efficiency due to the evaporation and condensation processes, which take place in the same enclosure at minimal temperature difference. Numerous researches have been investigated to enhance the performance and yield of the solar still by different modifications.

Advancements and research carried out in the solar desalination process enhance the yield and performance either by designing a new setup or by incorporating two or more techniques into a single setup. A solar still equipped with single slope, double slop, single basin, multi-basin, evacuated tubes, parabolic/spherical concentrator, etc. are the systems included as per the requirements of raising the temperature of the inlet temperature of saline water which will be evaporated for desalination. Optical Concentrators are the optical systems used to concentrate the diffused radiation at a single point or line to rise the temperature of the point to a substantially high degree. When heat transfer takes place to saline water, it raises the temperature to around 150°C. This high temperature associates an increased rate of evaporation, which in turn improves the yield of the process.

1.3.1 Solar still:

Solar still is a glass-enclosed apparatus used to trap solar radiation. It's the principle of working. It is based on first evaporation and then condensation. Solar energy is incident over the glass cover of the apparatus placed at the inclination (of the orientation with the Sun, for Delhi it is 27.7° N). This radiation energy is absorbed by the bed of the basin which is black painted to absorb maximum. This heat is used to evaporate the saline water. Vapour condenses at the glass cover ceiling and at the side surface due to temperature differences. This condensate is collected in a container, which is free from dissolved contaminants. This is a potable system that can be utilized to fulfill the needs of small scale utilities at the house hold level as it is limited to its size and efficiency. This system is less efficient as it works on a renewable energy source and its availability is not constant throughout the day. Recent advancements develop a lot more efficient apparatus with relatively high productivity rates. This system is easy to manufacture, maintain, ecofriendly and cost-effective.

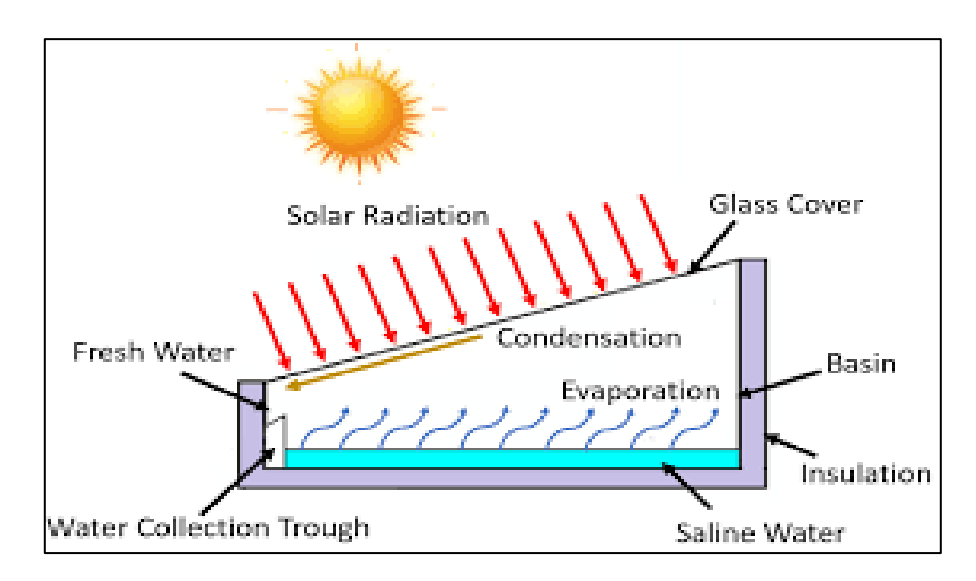


Fig. 1.8 Solar Still principle

A model is designed on two platforms, COMSOL Multi-physics and ANSYS and simulation is run to perform the analysis of the temperature variations in comparison to variation of irradiation, time variations for different regions of the triple basin system. Triple basin system is an improved design of basic solar still. It uses the heat collected by the evaporated fluid in the lower basin. Multi-layered system improves the thermal heat

utility and reduces losses which otherwise occur. This system is equipped with parabolic concentrator to guide the irradiation from its surface to collect at the surface of the triple basin chamber to be utilized to heat the fluid inside. Hence, this system includes parabolic concentrator with aluminium sheets coated on the inner surface of the reflector, a triple basin setup, outer fibre casing where at the upper surface the condensate is collected through the provision of the channels at the bottom end of the slope of ceiling. A lower surface of the basins is equipped with the provisions of fins to enhance the area heat transfer. These hollow fins can be filled with heat storage media like charcoal, sand etc so as to facilitate the energy supply during non-sunshine hours or otherwise.

CFD analysis of a system is a power tool to analyze a setup for its productivity and stress analysis. Modelling on COMSOL – Multi physics and ANSYS Space Claim software is done. Analysis of the system, including phase change space, concentrator space (reflector sheets), fins surface and filled material (charcoal), triple basin glass and outer casing, upper surface of casing ceiling, has been done on COMSOL - Multi physics and ANSYS.

Simulation modelling on COMSOL Multiphysics is performed to analyze the heat transfer and mass flow of the evaporation process of saline water. Srithar [30] experimentally analyzed the performance of triple basin desalination system equipped with parabolic concentrator. His system incorporates triangular fins to store energy during the sunshine hours so that some sort of desalination process can be carried out when in off sunshine hours. This helps in increasing the condensate and improving the efficiency of the system. Our system incorporates the same design, but the variation in the design of fins is carried out to analyze the results based on cylindrical fins. Cylindrical fins have slightly lower surface area, but the curved plane's symmetry facilitates the induction of irradiation on the surface, which facilitates the conductive and radiative heat transfer. It has been analyzed that the cylindrical fins produce a better heat-containing zone, which facilitates the smooth heat transfer phenomenon. Cylindrical fins causes improved heat transfer efficiency by 12% compared to heat transfer by triangular fins.

The utilization of solar energy as a thermal source of energy in desalinating seawater applications has been limited to small-scale utilities in rural areas. This is mainly because of its low efficiency and productivity as compared to high capital expenditure. However,

due to shortfall of availability of fossil fuels and the increasing demand for fresh water and increasing water demand for irrigation and drinking needs have resulted in the development of water purification and desalination through renewable sources of energy.

CHAPTER 2

LITRATURE REVIEW

Performance analysis was carried out by Phadatre et al. [3] experimentally to analyse the impact of water depth on the internal heat and mass transfer in a transparent plastic covered solar still, max. distillate output of $2.1 \text{L/m}^2/\text{day}$ was obtained with the depth of water in still basin 2 cm. Elango et al. [4], in this experimental analysis found that the productivity of single slope single basin and double slope double basin under two cases, with insulation and without insulation and decided that double slope double basin with insulation has more productivity.

Zurigat et al. [5] models a regenerative desalination unit with two layers of basins equipped with cover cooling arrangement over the second basin and employs the latent heat of vaporisation of the first effect to yield more in second effect. They concluded that the temperature difference obtained due to cooling arrangement improves the efficiency by 20%, perfect insulation by 2.5times and wind speed by 50% (for 0 to 10m/s). Kumar et al. [6] experimentally analyzed the establishment of cover cooling arrangement over concentric tubular solar water desalinating system. It was found that yield was increased by 50%, [3050ml/day] with air as cooling agent, 144% [5000ml/day] with water as cooling media as compared without such arrangement [2050 ml/day].

Rajaseenivasan et al. [7] comparative analysis on single basin SS with double basin SS arrangement and establish that double basin system is 84% more effective than single basin solar still. Rajaseenivasan et al. [8] experimentally analysed double slope single basin and single slope double basin and found that single slope double basin has 85% more efficiency than double slope single basin system.

Panchal et al. [9] attempted to enhance the double basin solar yield still with the provision of granite gravels and vacuum tubes. Three setups i.e. (a) double basin SS, (b) attached with vacuum tubes and granite gravels. The system was examined experimentally and

found that double basin with vacuum tubes and system coupled with vacuum tubes, granite gravels improves the distillate water by 56% and 65% respectively compared to double basin solar still alone. Rajaseenivasan et al. [10] perform review analysis on different systems to incorporate to improve the distillate and improve the efficiency and found certain arrangements such as double effect system is more efficient than single effect, provision for cooling water, multi-basin system, parabolic concentrators, vacuum tubes enhances the productivity & increases the efficiency of the system significantly.

Xiong et al. [11] performs an experiment on triple effect solar still arrangement equipped with vacuum tube collector involved with lower basin and found that the system forms a maximum yield of 43kg/day. Velmurugan et al. [12] perform an experiment to analyse the effect of incorporation of the fins at the lower side of base of the basin and found that the system's yield is has significant improvement i.e. increased from 1.88kg/ m² to 2.8kg/m². Sponges increase productivity by 15.3%, wick type SS improves it by 29.6%, fin-type solar still enhances the productivity by 45.5% when compared with conventional solar still.

Sebaii et al. [13] examined the fin parameters on the SS for productivity. He found that yield efficiency of the finned plate type solar still (FBLS) improves with increasing fins' height. Although thickness and number of fins give adverse effects when increased. Murugavel et al. [14] studied the performance parameters on double slope still with different wick materials and found that still with lightweight black cotton cloth form a better wick material than additional tested materials such as sponge sheet, cotton cloth, coir mate etc. still with rectangular aluminium fin enclosed with a cotton cloth in along its length pattern is more efficient.

Energy storing materials (ESM) are the materials that stores the energy when the source (sunlight in our case) is available and releases it when a source is absent (sunshine-off hours). Materials that can store sensible heat like iron scraps, red brick pieces, washed stones, cement concrete pieces, quartzite rock etc. Murugavel et al. [15] examined the effect of ESM and found that quartzite rock ³/₄ inch sized is effective heat storing material. Eltawil et al. [16] designed a system with a solar dish concentrator (SDC) with provision for preheating of brackish water and compared its results with simple solar still. They found that the yield of the system with SDC is 6.7 l/m²/day i.e. twice that of conventional still as 3

l/m²/day. Distillate production is found to be 347% higher when brackish water is preheated and without preheating, it is established to be 244% higher than conventional still.

Smith et al. [17] performed an experiment where inclined wick type SS couples the V-trough solar concentrator. They concluded that this arrangement significantly increases still efficiency and productivity. Denkenberger et al. [18] executed an experiment to study the influence of PCM i.e. phase change material, and on the productivity and efficiency on concentrator attached with hemispherical basin SS. They found that yield of the system with phase change material is increased by 26% in comparison to simple solar still.

Rajaseenivasan et al. [19] carried out exergy and performance analysis of double basin solar still equipped with diverse materials wrapped around basin to increase productivity and reduced thermal energy losses and improve heat storage capacity if the system. It has been found that basin equipped with mild steel pieces had max. exergy efficiency of 1.412% & 2.072% for single basin and double basin resp. Eltawil et al. [20] performed experimental analysis to evaluate the performance of a hybrid evacuated solar heater with desalination still to contain continuity in the distillate production. It was found that water production is enhanced by 114% over double-layered square wick still (DLSW). Distillate production has also been improved by 215% when brackish water is served during night time.

Rajaseenivasan et al. [21] carried out an experiment to analyze the effect of an integrated flat plate collector to heat up the saline water for desalination process. He divided the basin into 6 compartments so that the heating of segment is limited to small area compared to complete basin area at once. Thus his process outcomes state that the application of an integrated system and partition of the basin area improves the performance by 60%. Selvaganesan et al. [22] designed, fabricated and tested a solar adsorption system which considerably reduces the energy loss from the bottom of the basin thus improves efficiency and production of the system. Solar adsorption system consists of activated carbon-methanol integrated system. Sensible heat of vaporization is absorbed by activated carbon and latent heat of vaporization is absorbed by methanol. Circulation of water through the inner tube of adsorbent bed is sent to the basin, thus improving the evaporation rate during

daytime and later during sunshine hours. Improved distillate production is in the range of $3.1-4.3 \text{ kg/m}^2$ as compared to $1.9-2.3 \text{ kg/m}^2$ for simple solar still.

Velmurugan et al. [23] designed a stepped still and effluent settling tank and experimented on the performance enhancement due to these steps. They found that the rate of evaporation and condensate production is significantly improved by 53.3% when fins were installed in stepped still, 68% when sponge and pebble were incorporated, 98% combination of both arrangements is applied. Nishikawa et al. [24] developed triple effect evacuated solar desalination system, which uses steam energy from the previous stage to heat the subsequent stage and produce condensate at the end of each stage. Still developed is self-sustainable as it incorporates both solar collectors and solar cells. The evacuated system allows the water to evaporate at a lower temperature and triple-stage system reduces the thermal energy degradation and make the most out of the available energy at the end of each stage. Highest performance is obtained at 9.44 kg/m²/day for condensate production. It also produces 952.5 Wh/day of electricity.

Sebaii et al. [25] demonstrated a transient mathematical model for the solar still with triple basin setup. He found that the evaporation rate is maximum for the minimum mass of water at the surface of the basin without any dry spots and it decreases with increasing mass of water. He also found that the velocity of the air above the surface of water facilitates the rate of evaporation by a certain instant, but it is not dependent on the water mass in the lower and middle basin. Above that, there is no significant improvement in the rate of evaporation. Maximum distillate production in triple basin setup was calculated as 12.635 kg/m²/day, which justifies the result with experimental data. Jianyin et al. [26] carried out an experimental and numerical analysis for the multi-effect solar still where the application of staged trays of the corrugated pattern are utilized to improve the better utilisation of increased surface area to reduce the condensation resistance. Also, solar energy is supplied from evacuated tubes from the bottom and coated surface over the top efficiently. This combined effect of both the sources highly improves the efficiency of the system and improves the yield significantly. They also find out that the condensate yield is also produced during off sunshine hours, comprising of 40% of total yield, which is

significant. This highly depends on the starting temperature, higher starting temperature can produce the overall efficiency of the equipment to 91% and performance ratio of 1.86.

Feilizadeh et al. [27] performed an outdoor study on the performance evaluation of basin type multi-effect solar desalination system and the effect of a collector over basin area (CBA). System is incorporated by single, double, triple flat plate collectors of 3.45 m² each resp. They recorded the condensate production on an hourly basis for 24hrs a day. They found that a basin equipped with a single collector with CBA 3.45 m² produces 11.56 kg of distillate during the winter season. With double collectors, the yield is improved by 96%, and adding 3rd one causes the increase in production by 23% only. For the summer season, 48% and 23% are the improvements when adding second and third collectors respectively. Rajaseenivasan et al. [28] carried out performance study on solar still with square and circular fins on the basin surface when wick material is covered over fins. They found that the production of the system comes out to be 4.55kg/m²/day as compared to 3.16kg/m²/day for conventional solar still. They also carried out CO₂ mitigation analysis and found that 5.6 to 36.6 ton of CO₂ is mitigated for the lifetime of 5 to 30 years of operation.

Kabeel et al. [29] carried out cost analysis for a different set of solar still configurations depending on the productivity and cost of setup and maintenance. They found that maximum productivity (maximum daily and best average) and efficiency was produced for single slope pyramid shape solar still setup. 1533 l/m² of higher annual average production is carried out for the pyramid shaped solar still and per litre cost of condensate production is coming out to be approx. Rs. 1/L. whereas 250 l/m² is lowest annual average of production using modified solar still with sun tracking at about Rs. 17.20/L. Srithar et al. [30] experimentally analysed the triple basin solar desalination performance still (TBSS) with energy-storing material stored inside the triangular fins below top and middle basins. He also incorporates a cooling water arrangement as cover cooling (CC), parabolic dish concentrator (PDC), PV panel. He analysed the TBSS with CC, TBSS with PDC and TBSS with CC & PDC with charcoal and river sand filled in the triangular fins. TBSS with river sand and charcoal in fins improves the distillate production by 25.6% and 34.2% compared to conventional TBSS setup.

Setoodeh et al. [31] developed a three-dimensional model. In this model, a different phase method was used for the combined process of evaporation and condensation by the assist of a computational fluid dynamics simulation tool. Using this tool, a process of the simulation of single slope solar still was accomplished to get results. In the structure of a solar still, the volume of fluid (VOF) was owned to give liquid and prepared by combining the air, water, and vapour system at the quasi-steady-state condition. The building of geometry and meshing was prepared by using ANSYS Workbench 11. A simulation was done using tetrahedral meshing, and different meshing having a different number of elements were developed to calculate better results 32322, 47179, 64694, and 85315 cells. The energy and mass transfer concepts, continuity and momentum at steady-state condition was used for numerical modelling. As a result, it was predicted computational fluid dynamics is a piece of strong equipment for designing process, variables investigation, and can be used for removing difficulties during geometry creating of solar still. Khare et al. [32] created a multi-phase, 3D computational fluid dynamics model of simple solar still by using ANSYS FLUENT v14.0. and also experimented on it. The simulation and exploratory system of single slope solar still were compared with each other for the climate condition of Jaipur. The assist of ANSYS Workbench accomplished the physical structure surfaces and its meshing. The meshing of geometry has 3D hexahedral shape elements and 1.5 million elements were created during meshing with a growth rate of 1.2. The energy and mass transfer concepts, continuity, and momentum for the steady-state condition was used for numerical modelling with some assumptions. In a simulation, it was checked the overall efficiency and other parameters.

Panchal et al. [33] performed an experimental and computational fluid dynamics modelling of the single-slope solar still. The Geometry was prepared using ANSYS Workbench 10 and unstructured tetrahedron mesh was used to predict the results. The simulation shows the consequences of water production, water temperature, and heat transfer coefficients using ANSYS CFX 10. Maheshwari et al. [34] were prepared a geometry of a double slope single-basin solar still, which was modelled by using solid works, and meshing was done using ANSYS ICEM computational fluid dynamics which consists of 170791 elements. The simulation was done using ANSYS CFX 14.0 to check the production rate and

temperature of the water. As a result, it was predicted overall production is maximum in March and November.

Fathy et al. [35] experimented with double-slope single basin solar still which was coupled with parabolic trough collectors (PTC) for increasing heat transfer. The solar radiation incidents upon the parabolic trough collector, which transfers its temperature to the oil finned-serpentine loop heat exchanger. Results of Solar still linked with parabolic trough collectors (PTC) were contrasted from the conventional solar still, which showed the yield of solar still raises by lessening salted water deepness and it also raises by using parabolic trough collectors. The result shows every day, pure water outputs at 20 mm salted water deepness is measured 4.51 and 2.31kg/m² for conventional solar still and 10.93 and 5.11 kg/m² for solar still with parabolic trough collector. Madhlopa et al. [36] performed research for determining the solar irradiance outflow in single-slope solar still with the help of outside and inside reflectors. In the model, two variables were supposed to estimate, are the reflectance and vision view factor of surfaces. This work was accomplished for single-slope solar still and another for a solar still using a separate condenser. From the results of both still, it was analysed that conventional solar still produces a maximum value of distillate yield than solar still joined from the condenser.

Panchal et al. [37] experimented for the analysis of different materials of absorber sheets to check the working of double-slope solar still. This experiment was done to increase the temperature inside the still. It was analysed that the copper plate has a high value of temperature compared with galvanized iron and a mild steel plate on account of the higher thermal conductivity of copper. Tripathi et al. [38] performed experimental works to check the influence of different salted water deepness in the container for heat and mass transfer coefficients for single-slope solar still. A variation of heat transfer coefficients with depth was noticed and the internal convective heat coefficient lessens with water deepness because of the lessening in temperature of the water. It was observed that the vaporized heat transfer coefficient raised to 0.15 depth.

Badran et al. [39] experimented on single slope solar still. The experiment was performed to evaluate the yield of single slope solar still using asphalt and without utilizing the asphalt. The utilization of asphalt in the basin results in a growth of 29% in output and

remarked that the combination of the sprinkler with asphalt was additional effectual than asphalt. Singh et al. [40] experimented on single slope solar still and examined it for the finer inclination angle for production. For this analysis, a covered setup was designed at different inclined angles of 15°, 30°, and 45° separately. The consequences of the single-slope still were contrasted with Dunkle's model and data was matched. Consequences give the details that the high evaporation was checked at 45° and the lowest at 15°. The conclusion shows that a rising in inclined angle, vaporization rate, and the temperature difference on either side of the glass inner surface and watering layer increase and have a higher output than Dunkle's model.

Gokilavani et al. [41] made a model of conventional solar distillation experimentally and also prepared a model by using ANSYS Workbench 14.5 and simulated in ANSYS CFX. The work of the experiment was compared with the simulated study and verified the temperature values over the glass on 27/Nov/2013 and 28/Nov/2013. The result shows the maximum temperature achieved inside the glass and glass temperature on 27/Nov/2013 compared to 28/Nov/2013.

Singh et al. [42] researched single-slope solar still for obtaining the desired inclined angle to obtain the superior output. The geometry was prepared in ANSYS CAD module and then transferred to ANSYS meshing module for meshing making. Simulation work is completed by ANSYS CFX 13. Boundary condition was used for decoding momentum and energy equation. In the still, two condensing glass covers have 15° and 30° slopes. A simulation was done to get a temperature difference between 40° and 60° at an interval of 2°C for output. Adhesive forces are used to evaluate water spheroid on the glass sheet and 30° inclined to condense cover to get the highest use of the heat transfer coefficient of convective and evaporative. The 30° inclined condensing cover provides a maximum production efficiency of 29.4% than 15° slope.

Bhaisare et al. [43] developed a computational fluid dynamics model of double slope single basin solar still for the Gorewada water purification plant, Nagpur. The geometry was prepared in ANSYS workbench and then transferred to ANSYS meshing. The simulation result was obtained by using ANSYS 16.0v. As a result, it was analysed, the maximum heat flux decreases concerning time, i.e., 9.1054e+005 to 2.0565e+005 in 1 sec and also

predicted maximum temperature remains constant and minimum temperature varies with time. Badusha et al. [44] developed a two-phase 3D structure with the help of ANSYS. Still was prepared for the process of evaporation-condensation in solar still with the help of computational fluid dynamics. It was better by either side of the simulation consequences and the experimental consequences with some misconception. The result estimated using ANSYS CFX shows a powerful method for geometry creating, variable estimation, and trouble removal in solar still building.

Thakur et al. [45] accomplished modelling work by computational fluid dynamics tools and experimented with single slope solar still. The geometry was created and then imported for meshing in ANSYS meshing with a minimum grid size of 4 mm and 10 mm to achieve better results. The meshing geometry has several nodes 632088 and a total number of elements 553048. The computational work was done for optimizing the different water depths of solar still i.e., 0.01, 0.02, and 0.03 m. and the meshing type was hexahedral. The result is acquired by computational fluid dynamics work and showed better accordance between exploratory work and simulation work. It was remarked that the optimum depth for the better output was 0.01m. Panchal et al. [46] experimented and worked on CFD to create a structure of solar still. For raising the absorption of solar radiation, an experiment of single slope solar still was performed that is accompanied by a black layer at the base of the solar still. The simulation of geometry was done in ANSYS CFD 11. The depth of water of the experiment still was 40 cm in clear sky condition. There were four thermocouples used to collect the data. Both simulation and experimental results were compared with each other.

Sampathkumar et al. [47] accomplished a thorough review of single-slope solar still. For enhancing output, a single slope was joined with evacuated tube collector. Accompanied by the collector, solar still works as a merge system. This work was done for different timings of different days. Evacuated tubes coupled solar still provide a rising productivity of 77% with a temperature increment of about 60°C than simple still. The conclusion signifies that there is better accordance between the simulation consequences and the exploratory consequences with some misconception. Tabrizi et al. [48] did an exploratory analysis on single slope solar still with a built-in sandy tank beneath the basin liner as a storage

medium. The integrated heat reservoir produces far up solar still output at the nights and cloudy days. For water injection in solar still, it doesn't need a pumping system. For increasing the accuracy in temperatures, the glass temperature was checked at 12 nodes. The results of solar still visualize that the use of a sandy heat reservoir to a solar basin still increases daily output.

Tripathi et al.[49] worked on a simulation structure for thermal analysis of single-slope solar still by considering the variables of the solar fraction. The geometry of the two-phase 3D structure was designed in AUTOCAD 2000. The system measurements were 1 m \times 1 m area with 10.2° slope of the glass cover. The experiment was conducted for New Delhi weather conditions (27.0238° N, 74.2179° E). A MATLAB program was used to calculate convective and evaporative heat transfer coefficients and also estimated sun irradiance. There was better accordance between the simulation consequences and the exploratory consequences with some misconception and theoretical estimation at the time of the day as a contrasting night.

Concentrator thermal efficiency is established by Bellos et al. [72] using some arbitrary constants and variables along with some assumptions based on the geographical and geometry parameters and is given as,

Optical Efficiency of concentrator is given by,
$$\eta_{opt} = \frac{Qu + Qloss}{Os}$$
,

Concentrator efficiency,
$$\eta_c = K \times \frac{T_{in}^4 - T_{am}^4}{A_a - G_h}$$

where, Q_u is available useful energy, Q_{loss} is heat lost to surroundings and Q_s is direct beam solar irradiation, T_{in} & T_{am} are inlet and ambient temperatures.

Tiwari et al. [50] experimented with single slope solar still which was linked with a flat plate collector. A trial was done to assess the temperature of inside and outside glass and its influences on yields. A numerical simulation was executed for the weather condition of New Delhi (27.0238° N, 74.2179° E) and also at the height of 216 m greater than the averaged sea status. The variables attached in the investigation were the broadness of the cooling casing, collector absorbing surface, wind velocity, and water deepness of the still. Dissimilar condensing cover materials were used, whose names are copper, glass, and

plastic. The consequence shows that the maximum value of thermal conductivity of copper and minimum deepness are important variables for increasing production. Copper gave higher productivity compared to other materials. The conclusion shows that inside glass temperature shows an important role in estimating production. Per day production is finer for the active system as a contrast to the passive system.

Mishra et al. [51] researched to work for single slope solar still to improve productivity. Different methods and modifications were used for improving productivity. Some additional heat absorbers were added to increase productivity, namely gravel, sponge cubes, rubber, glass balls, charcoal, coating absorber aluminium sheet, dyes, and ink in the solar still. The maximum output depends on the surface of the glass sheet, absorber material, and vaporizing layer was 34.7, 40.6, and 7.96 kg m⁻²d⁻¹ individually, and maximum efficiency was recorded 3.5. The conclusion shows that solar production still lessens as it gains in the deepness of water in daylight and the output of wire-type solar still is roughly 20% more.

The objective of the study is to create a three-dimensional computational fluid dynamics model of triple basin solar desalination system equipped with parabolic concentrator to check the evaporation and condensation processes within solar stills at the climate conditions of Delhi (27.0238° N, 74.2179° E). Both models were developed using ANSYS Workbench and simulation works were done with the help of ANSYS FLUENT V19.2. All variables inside both solar still were calculated and examined at each stage. And it is also examined water production of the single and double slope of both systems for the entire day of 21 June 2020.

CHAPTER 3

METHODOLOGY

Experimental Setup:

Two different two-phase 3D models were designed in the volume of fluid of the multiphase phase model. Both stills were also developed using evaporation and condensation processes at transient conditions, which explains that only vaporization of liquid occurred at the surface and their interface was considered for modelling. The act of solar stills is dependent on different parametric variables such as coefficients of internal heat and mass transfer, are checked. The mass transfer coefficient and internal heat in solar still are dependent on convection, evaporation and radiation. In consequence, the convective HT coefficient, evaporative HT coefficient and radiative HT coefficient are for the heat transfer coefficient. An RNG k-ε turbulence model was applied with standard wall functions for both phases. The time, volume- average continuity, mass transfer and energy equations were found numerically in this project for each phase.

3.1 Governing Equations:

Model equations that obey steady-state conditions are dependent on momentum, energy, continuity, and mass transfer conservation concepts.

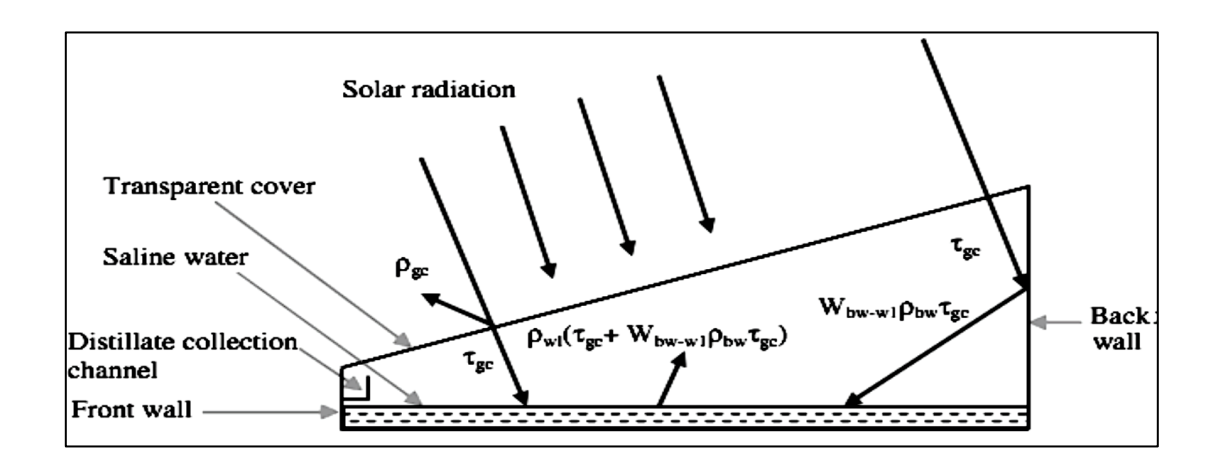


Fig 3.1 The single slope solar basin [9]

3.1.1 Energy Equations:

The assumptions of energy balance equations are:

- 1. Basin water and inside-glass surface of solar still has no increase in temperature.
- 2. No escaping of water from any type of hole or crack is present in the solar stills.
- 3. The water level is kept constant inside the basin.
- 4. The heat capacity of the glass surface, absorber, and the insulated material is very low.

The energy equation of the mixture is mentioned underneath,

$$\frac{\partial}{\partial t} \sum_{k=1}^{n} (a_k \rho_k E_k) + \nabla \cdot \sum_{k=1}^{n} \{ a_k \bar{v}_k \left(\rho_k E_k + p \right) \} = \nabla \cdot \left(k_{eff} \nabla T \right) + S_E \tag{1}$$

where k_{eff} is the effective conductivity $(a_k(k_k + k_t),$

3.1.2 Continuity Equation:

$$\frac{\partial}{\partial t}(\rho_m) + \nabla \cdot (\rho_m \overline{\nu_m}) = 0$$
where $\overline{\nu_m} = \frac{\sum_{k=1}^n a_k \rho_k \overline{\nu_k}}{\rho_m}$ (2)

3.1.3 Momentum Equation:

The momentum equation of all phases is achieved by combining each equation of momentum of all phases.

$$\frac{d}{dt}(\rho_{m}\bar{v}_{m}) + \nabla(\rho_{m}\bar{v}_{m}\bar{v}_{m}) =$$

$$-\nabla p + \nabla[\mu_{m}(\nabla\bar{v}_{m} + \nabla v_{m}^{T})] + \rho_{m}\bar{g} + \bar{F} + \nabla(\sum_{k=1}^{n} a_{k} \rho_{k}\bar{v}_{dr,k} \cdot \bar{v}_{dr,k})$$
(3)

 ρ_m = Density of mixture

 \overline{F} = The gravitational body force and external body forces

 μ_m = molecular viscosity of the mixture

3.1.4 Volume Conservation Equation:

It is a constraint which shows the unity of volume fractions by adding:

$$r_G + r_L = 1 \tag{4}$$

 r_G = volume fraction of gas.

 r_L = volume fraction of liquid.

3.1.5 Mass Transfer Equation:

The enthalpy sources in a system for different phases are:

$$H_p = -m_p i_q j(h_p^i) \tag{5}$$

$$Hq = m_{p^i q} j \left(h_p^i + h_p^{f^i} - h_q^{f^j} \right) \tag{6}$$

3.1.6 Pressure Constraint:

The gas phase and liquid phase share the same pressure field:

$$P_G = P_L = P \tag{7}$$

3.1.7 Heat Transfer Equation:

The buoyancy force is the primary cause of heat transfer. The heat transfer coefficient that has evaporative, radiative, and convective across the contact and the gas phase was prepared with the help of the null equation model and the liquid phase is demonstrated by,

$$h_{total} = h_{r\omega} + h_{cw} + h_{e\omega} \tag{8}$$

$$h_{Cw} = 0.8840 (Tw - Tg + \frac{(P_{\omega} - p_g)(T_w + 273)}{268 \cdot 9 \times 10^3 - P_w})^{1/3}$$
where, $P_w = exp\left(25.317 - \frac{5144}{T_w + 273}\right)$

where
$$Pg = \exp\left(25317 - \frac{5144}{Tg + 273}\right)$$

$$h_{e\omega} = 16.273 \times 10^{-3} h_{Cw} \cdot \frac{P_{\omega} - P_g}{T_w - T_g} \tag{9}$$

And,

$$\begin{split} h_{rw} &= \varepsilon_{eff} \sigma [(TW+273)^2 + (Tg+273)^2 (Tw+Tg+546)] \\ \text{where, } \varepsilon_{eff} &= \frac{1}{\varepsilon_g} + \frac{1}{\varepsilon_\omega} - 1 \end{split}$$

3.1.8 Water Production:

Defined contact mass flux was used for mass transfer models.

Assumption of water production:-

The rate of freshwater production is equivalent to the rate of vaporization of the water. So, the rate of vaporization of the water shows water production.

Hence, the equation of mass flux between the two different phases are:-

$$\dot{m}_{ew} = \frac{\dot{q}_{ew} \cdot A_w \cdot t}{h_{fg}} \tag{11}$$

where,

$$h_{fg} = 2 \cdot 4935 \times 10^{6} [1 - 9.4779 \times 10^{-4} T + 1.3132 \times 10^{-7} T^{2} - 4.7974 \times 10^{-9} T^{3}]$$

$$\dot{q}_{ew} = h_{ew} (T_{w} - T_{g})$$

3.1.9 Solar Irradiance:

 $\delta = 23 \cdot 45 \sin(360 * (n + 284) / 365)$

$$\omega = (solar\ time - 12:00) \times 15$$
where,
$$Solar\ time = Standard\ time \pm 4(L_{st} - L_{L_0ca}) + E$$

$$Ig = I_b + I_d$$
where, $I_b = I_{bn}\cos\theta_z$ and, $Ig = I_{bn}\cos\theta_z + I_d$ (12)

3.1.10 Convergence Criterion:

Newton-Raphson Method is used as a convergence criteria which is most widely used scheme. Let a function f(x),

$$x_{n+1} = x_n - \frac{1}{f'(x_n)} f(x_n)$$

Non-linear Equation, $f(x) = 0 \Leftrightarrow x = g(x)$

Convergence Criteria, use Lipschitz condition & $x_n = g(x_{n-1})$

$$|g'(x_n)| < k < 1 \Rightarrow |x_n - x^e| \le k |x_{n-1} - x^e|$$

Fast convergence, $|g'(x^e)| = 0$

$$g(x) = x + h(x)f(x), h(x) \neq 0$$

$$g'(x^e) = 1 + h(x^e)f'(x^e) + h'(x^e)f(x^e)$$

$$= 1 + h(x^e)f'(x^e)$$

$$g'(x^e) = 0 \Rightarrow h(x) = -\frac{1}{f'(x)}$$

Newton Rapson Iteration, $x_{n+1} = g(x_n) = x_n - \frac{f(x_n)}{f'(x_n)}$

This function shows quadratic convergence.

3.2 Computational Fluid Dynamics Model of Modeling:

Computational Fluid Dynamics (Computational Fluid Dynamics) is a valuable tool that has been used to examine and inspected the fluid flow repeated method of moisturized air and temperature variation near the walls. For visualizing the flow filed any location, computational fluid dynamics can be utilized to prepare the design, get the controlling step, and guide. In the study, computational fluid dynamics is utilized to create geometry, and the simulation result is obtained by using ANSYS 19.2v.

Proposed system consists of triple basin solar still (TBSS), parabolic dish concentrator (PDC), and cover cooling arrangement (CC), triangular/cylindrical fins incorporated below the top and middle basins as main components. Design details and parameters are mentioned below:

3.2.1 Geometry Creation:

Ansys is a beneficial engineering simulation software that is mostly used to solve engineering problems and make them more optimized. Figure 12 show the 3D geometry of tripple basin solar desalination setup with parabolic concentrator, which were modeled using Ansys Design modeler in Ansys 19.2.

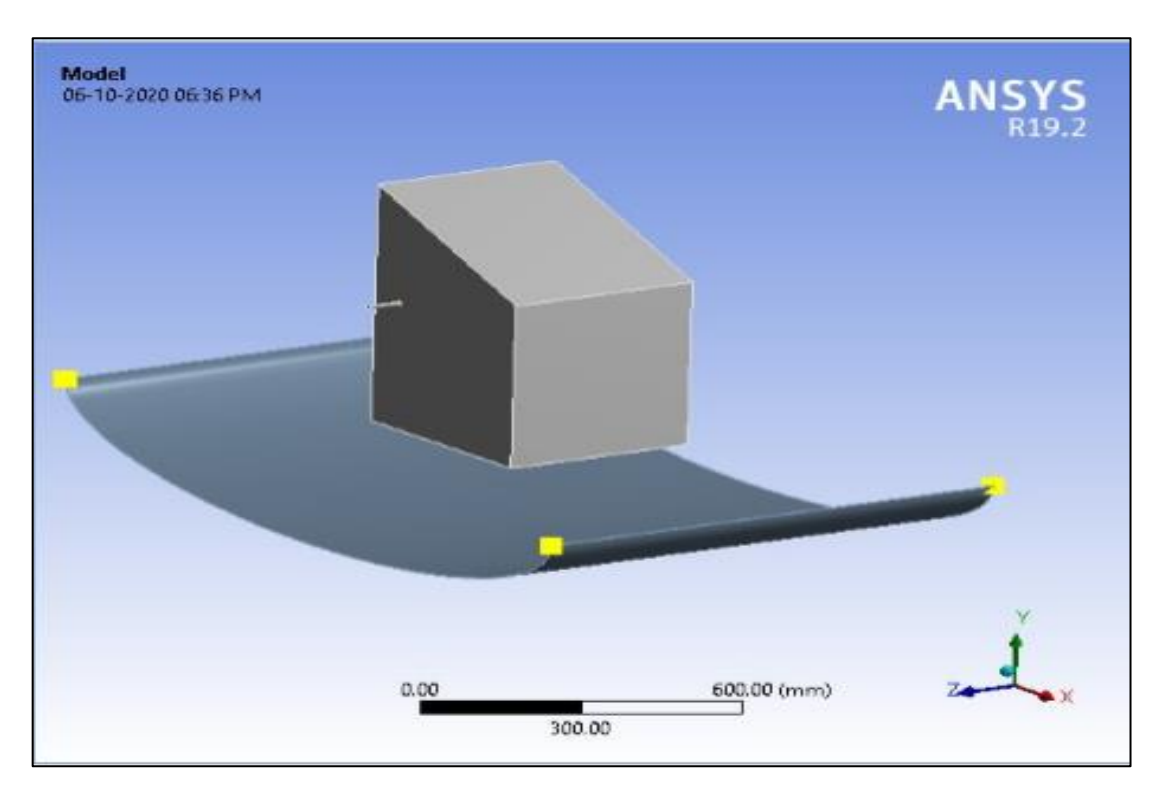


Fig 3.2 Triple basin solar desalination model

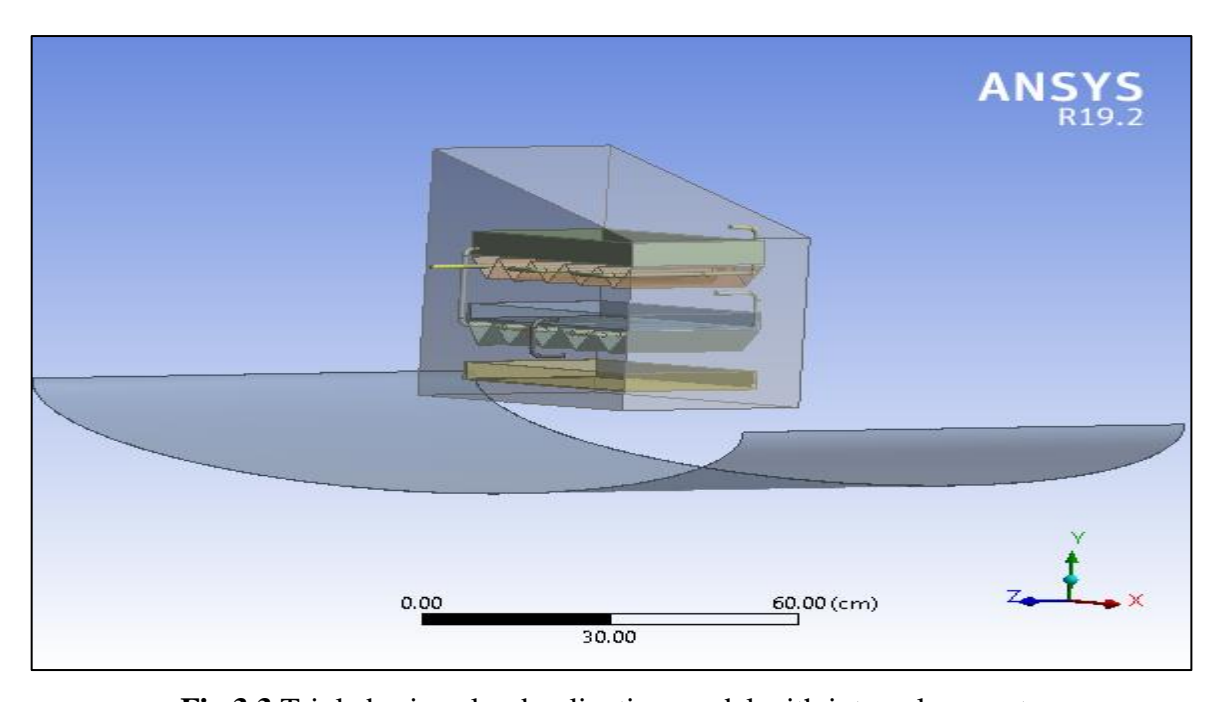


Fig 3.3 Triple basin solar desalination model with internal geometry

This model contains a concentrator, triple basins separated in compartments at top, middle and lower. Upper and middle basins contain triangular fins and pipes to flow saline water through them. This system is modelled as per dimensions.

Geometry:

Table 3.1 Geometry and properties

Bounding Box:							
Length	X = 1601 mm	Y = 781.21 mm	Z = 1000 mm				
Properties							
Volume 9.1139e+007 mm³		Scale Factor Value: 1					
Statistics							
Statistics Bodies 15		Active Bodies 15	Nodes 542951 Elements 2878069				

3.2.2 Parabolic Dish Concentrator (PDC):

A parabolic concentrator coupled with triple basin arrangement can concentrate the irradiation to the TBSS and thus improve the collection of solar energy. With the help of the concentrator the temperature of the water can reach 85°C [30]. Polished aluminum sheet of 1mm thickness is used as a reflective surface of the dish concentrator. Parabolic dish concentrator has a diameter of 1.25m and its focal length is modelled at 0.5m. Triple basin setup inside outer casing is mounted over dish concentrator with glass stands. This concentrator is mounted on the stand, which is manually adjusted by locking nut mechanism.

3.2.3 Triple basin solar still (TBSS):

This setup incorporates two components, one evaporative unit (inner component) and the other a condensing casing (outer glass cover- outer component). All the parts of the triple basin setup are modeled for 4mm thickness and the material is selected as window glass

sheet. This glass sheet facilitates the radiation to be captured from the top and sides. Dimensions of the inner component are selected as 0.3mX0.36m and 0.33m height. Inner component is divided into three basins with 0.12m gap in-between.

Top and middle basins carry 4 triangular/cylindrical hollow fins of 0.075m width and height of 0.05m (0.075m diameter for cylindrical fins when 4 fins are modeled). These fins were faded with charcoal and river sand in the hollow cavity to act as heat storage media. Copper pipes feed water through the fins of upper basin. Heat storage media helps the increased rate of evaporation during sunshine hours with better efficiency and intensity. Also, it facilitates evaporation during off sunshine hours. Constant level of feed water is maintained at 0.01m in each basin with overflow protection mechanism. Overflow water is carried away to successive steps (upper basin to middle basin, middle basin to lower basin) with the copper piping's via fins. Outer casing is modeled with 0.4X0.46m² with 0.4m height at one end and 0.62m at the other end with the angle of inclination at 28.7⁰ (latitude of Delhi, coordinates of Delhi Technological University campus).

Condensation occurs at both the surfaces, the top surface, and at the side cover of the outer casing. Thus channels to collect the condensate are attached on the side also covers along with the edge of the inclination. The cover cooling arrangement is also designed to increase the temperature difference between the vapor and glass sheet. This facilitates an increase in the rate of condensation. Thus, more condensate is produced.

3.2.4 Cover cooling (CC):

The cover cooling arrangement is incorporated in the design to facilitate increased temperature difference between the glass cover and the vapor. A CC arrangement consists of a pipe of 0.46m length with holes at regular intervals to facilitate the flow of cooling water over the entire cover surface. Cooling water is feed from the storage tank directly through the pipe arrangement and circulation is carried out by small pump getting power from the solar panel.

3.2.5 Meshing:

The physical model of the system was then meshed by using ANSYS 19.2 workbench Meshing. Fig 11(a) shows an unstructured mesh of triple basin setup, consisting of 2878069

elements and 542951 nodes at a growth rate of 1.2 and element size 10mm using 3D tetrahedral meshing at the basins and outer cover. At the same time, the concentrator has the hexagonal meshing pattern.

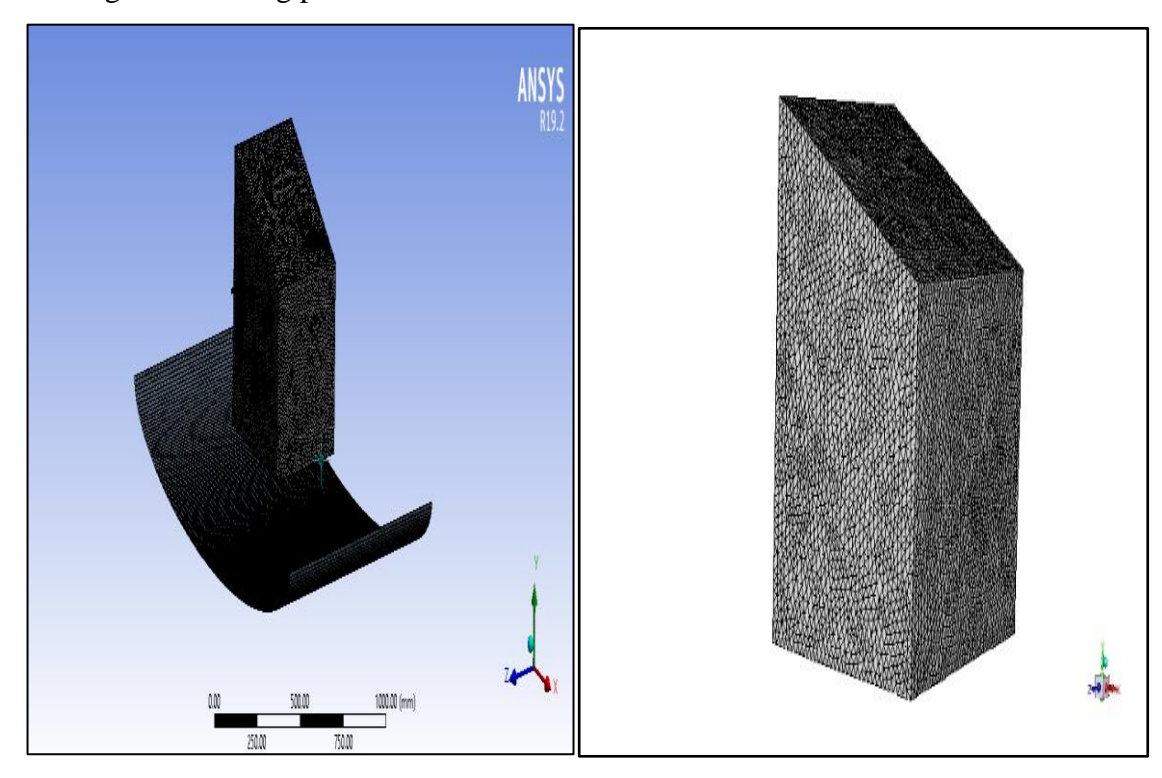


Fig 3.4 The unstructured mesh of triple basin setup and concentrator

3.2.6 Boundary Conditions And Initial Conditions:

Meshing files of triple basin stills are transferred to ANSYS FLUENT. A multiple phase structure of solar desalination still was prepared inside the volume of fluid (VOF) framework for water in the liquid state and a mixture of water vapor and air system at the transient condition with gravitational acceleration. Solar irradiance falls on the tapered glass surface of the outer casing glass cover is an important factor for the inner side of the setup, dependent on the transmissivity and absorptivity of the glass cover. First of all, solar rays incident over the glass surface and then absorbed by an absorber surface. This process raises the temperature of the water in the basin. In the fluent, physics and boundary conditions are specified to solve the continuity equation, momentum equation, and energy equation at all the boundaries. The RNG k-ε viscous model was used, which predicts the spread of flow and better water production performance. In the model, the near-wall

conditions were dealt with using 'standard wall function'. Adhesion forces are taken for producing droplets inside the solar stills. No-slip wall boundary conditions were defined for both the gas phase and liquid phase. The volume fraction of the water and air were taken as 0.13 and 0.87. Computational fluid dynamics simulation had a run time of 12 hours for this triple basin setup.

 Table 3.2: Boundary conditions for the simulation process

Domain	Domain type	Location	Boundary	Boundary details	
			type		
Solid	Cell	Absorber plate	Wall	Stationary wall with heat	
				flux	
		Glass cover	Wall	Fixed wall Temperature	
		Sidewalls	Wall	Adiabatic	
		Front and back	Wall	Adiabatic	
		wall			

CHAPTER 4

RESULT AND DISCUSSION

In this study, simulation results were calculated at fair weather conditions and each stage of both stills using ANSYS FLUENT v19.2. In Simulation results, the temperature distribution inside the still is examined and predicted the temperature of still for the entire day. The system is also validated for the number of fins installed and its geometry i.e. 4 fins of triangular nature and 4 fins for the cylindrical geometry are analyzed.

4.1. Simulation Results:

ANSYS FLUENT v19.2 was employed to check the results using 3.0 GHz CPU processors as parallel run with double precision. Fluent uses a second-order upwind solution process to transform the prevailing equations into a numerically resolvable algebraic equation.

4.2. Temperature Distribution:

Fig. 15 and 16 respectively visualize the gas-phase temperature volume rendering inside the TBSS pipes and basin. Temperature variation at each stage was calculated inside the apparatus. In the temperature volume rendering, the red colour visualizes the maximum value of the temperature, while the blue colour visualizes the minimum value of the temperature for triple basin system.

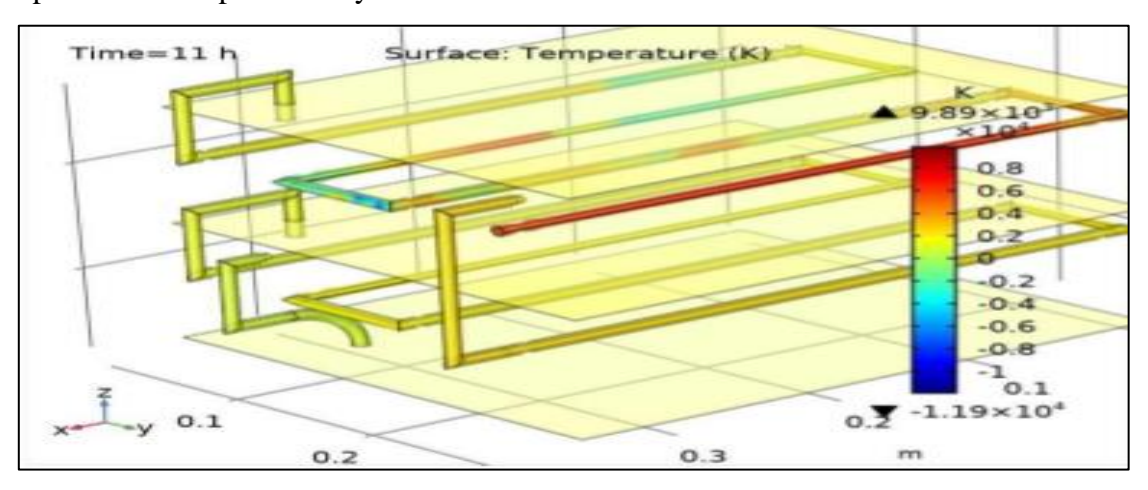


Fig 4.1 Temperature distribution inside the pipes and water surface

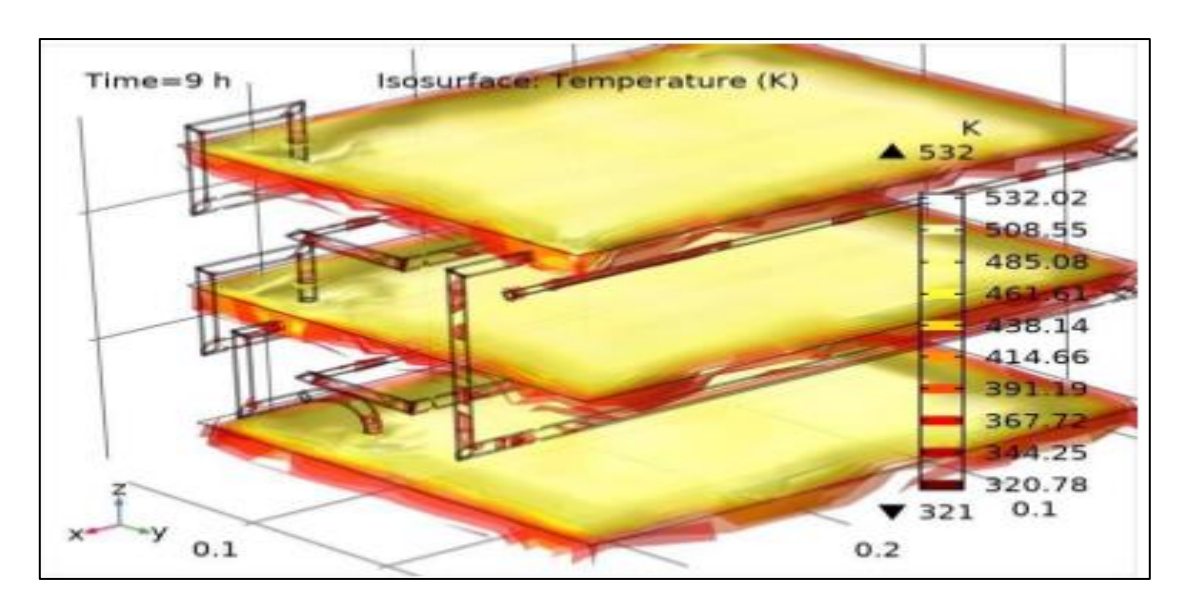


Fig 4.2 Iso-surface Temperature distribution inside the pipes and water surface

Fig. 17 and 18 respectively visualize the temperature distribution rendering inside the fins of triangular and cylindrical geometries. Maximum temperature inside the triangular fins is found out to be 73.112 °C and minimum is 22°C. Maximum temperature is distributed at the narrow edges of the triangular fins. Maximum temperature inside the cylindrical fins is found out to be 66.093 °C and the minimum is 23.438 °C. Maximum temperature is distributed at the lower surface of the cylindrical fins.

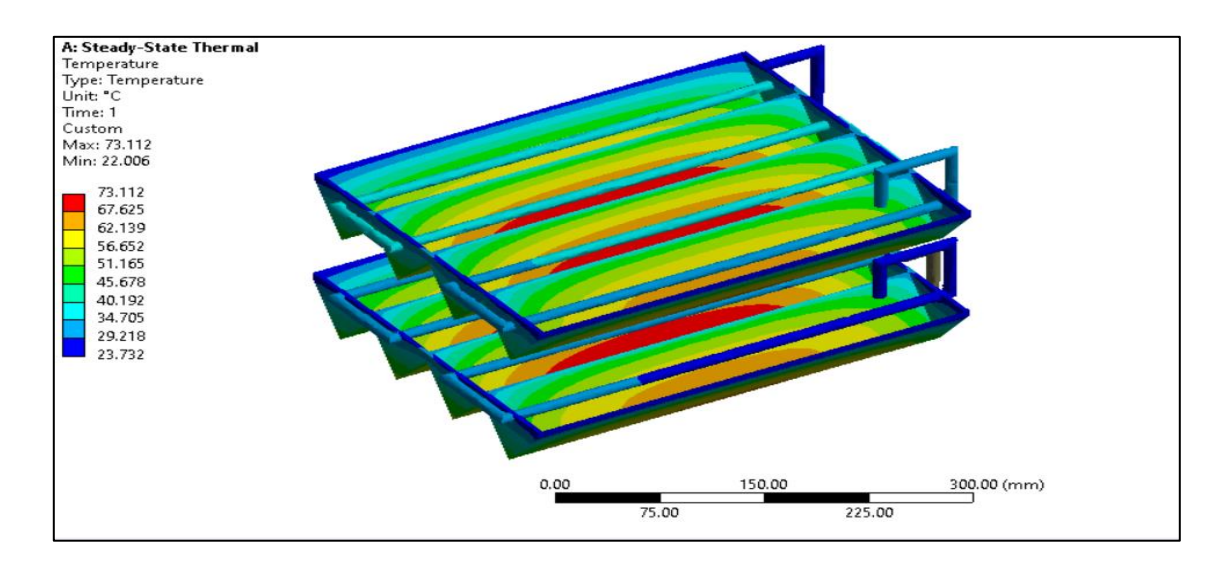


Fig 4.3 Temperature distribution of 4 triangular fins

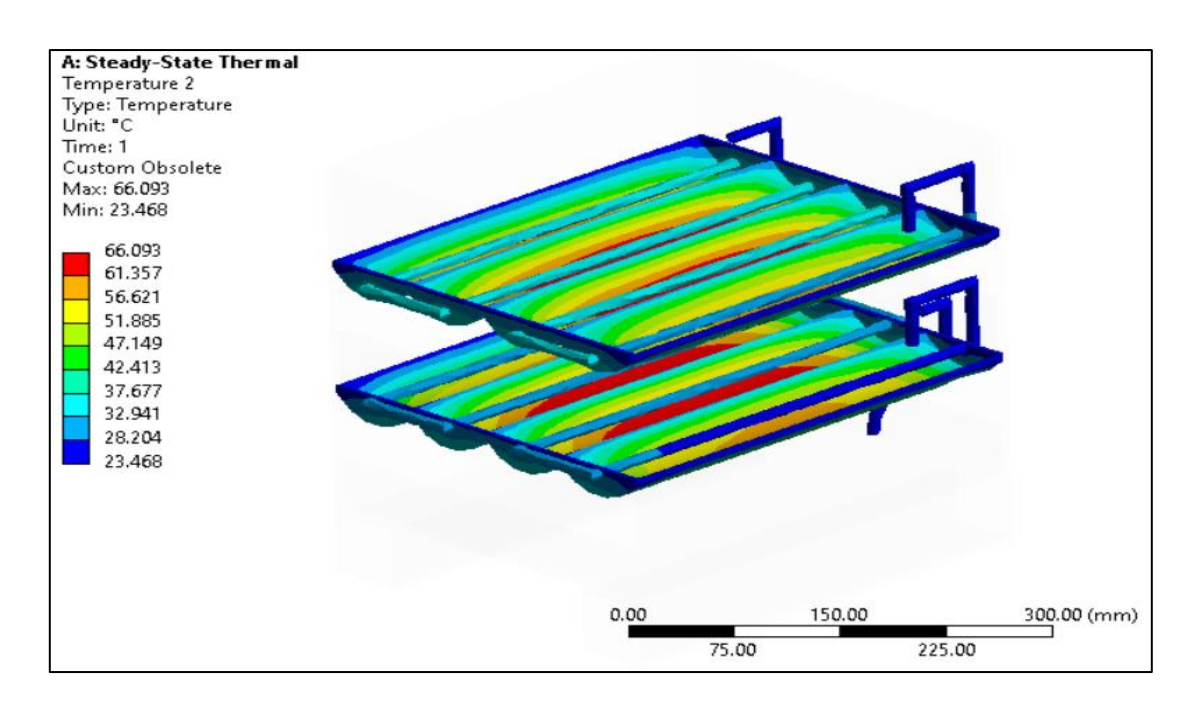


Fig 4.4. Temperature distribution of 4 Cylindrical fins

Fig 19 and 20 respectively show the irradiation heat flux falling on the surface

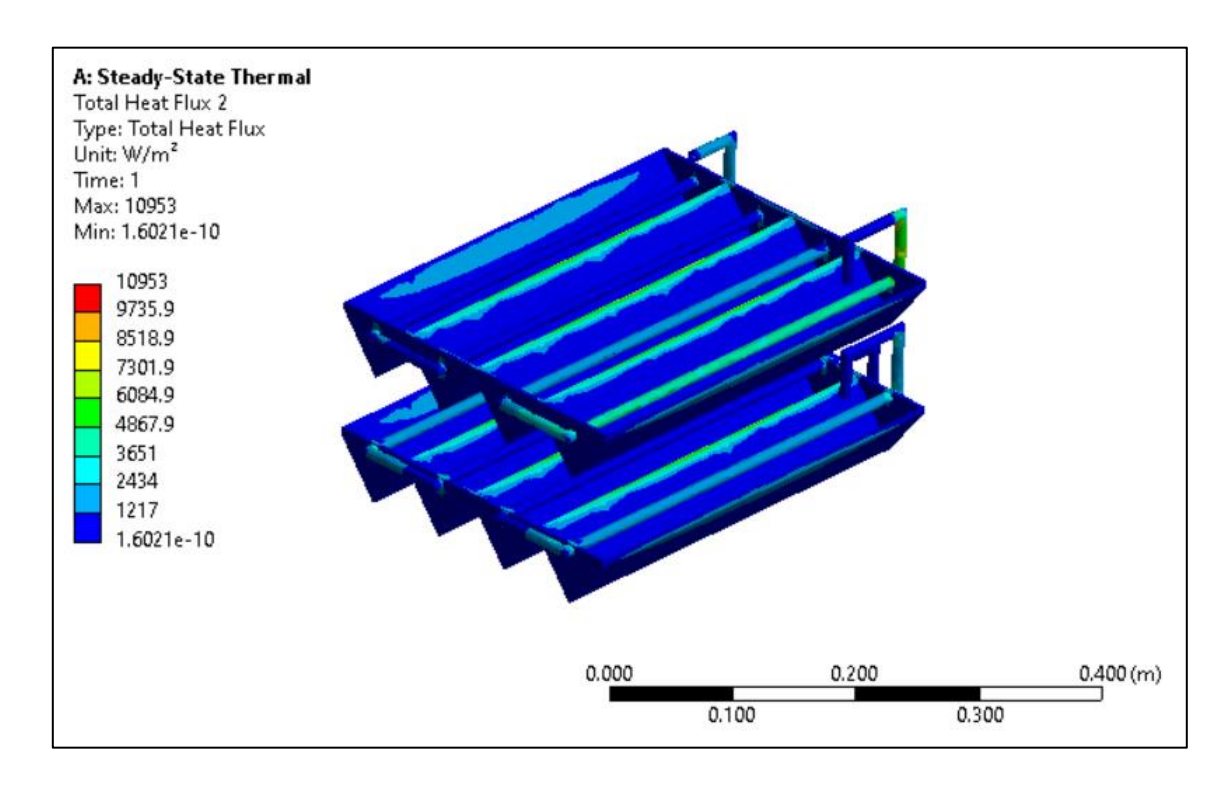


Fig 4.5 Irradiation heat flux distribution of 4 Triangular fins

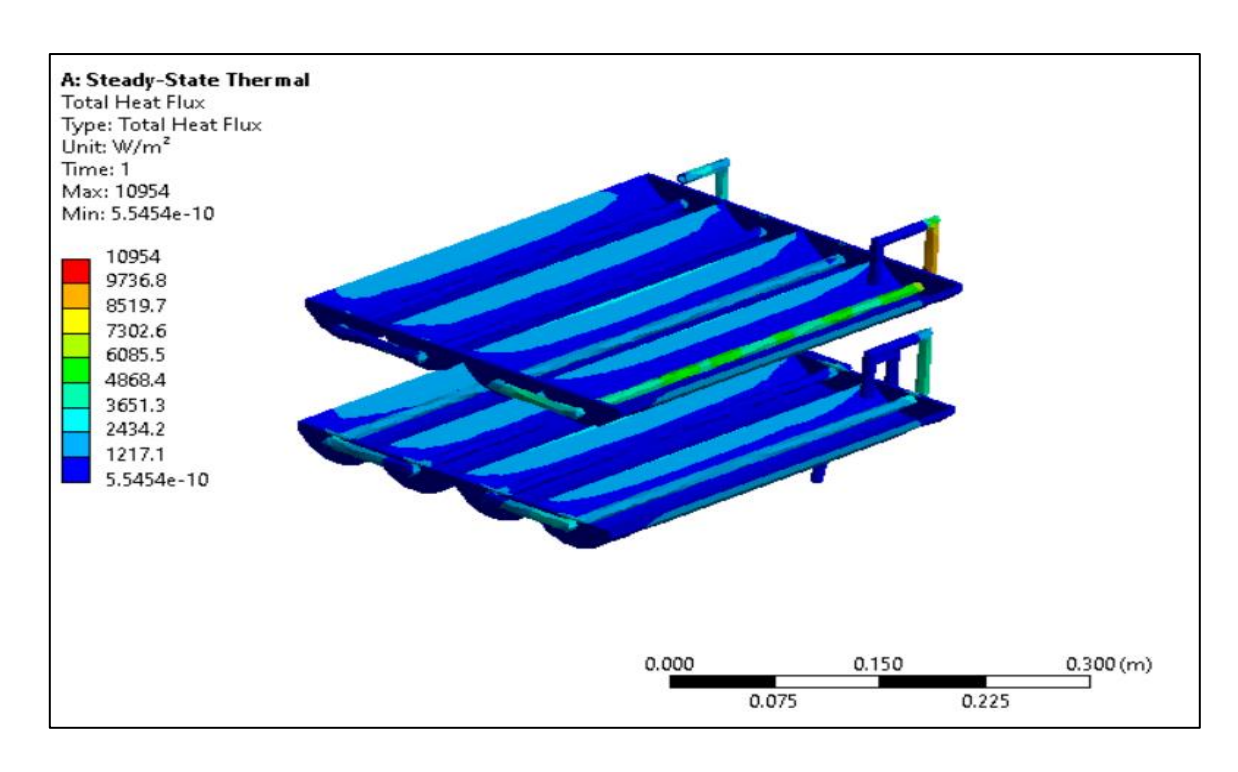


Fig 4.6 Irradiation heat flux distribution of 4 cylindrical fins

Comparison: peak temperature is higher in triangular fins than cylindrical fins as shown in the table below, but it is visible that the highest temperature is found at the edge of the fin in triangular fins. It should be noted that the cylindrical fins contain symmetry pattern; thus distribution of temperature is more symmetric and can be extracted through the pipes more symmetrically.

Table 4.1 Peak Temperature comparison for triangular and cylindrical fins.

Fins	Triangular Fins-4	Cylindrical Fins-4
Temperature	73.112	66.09

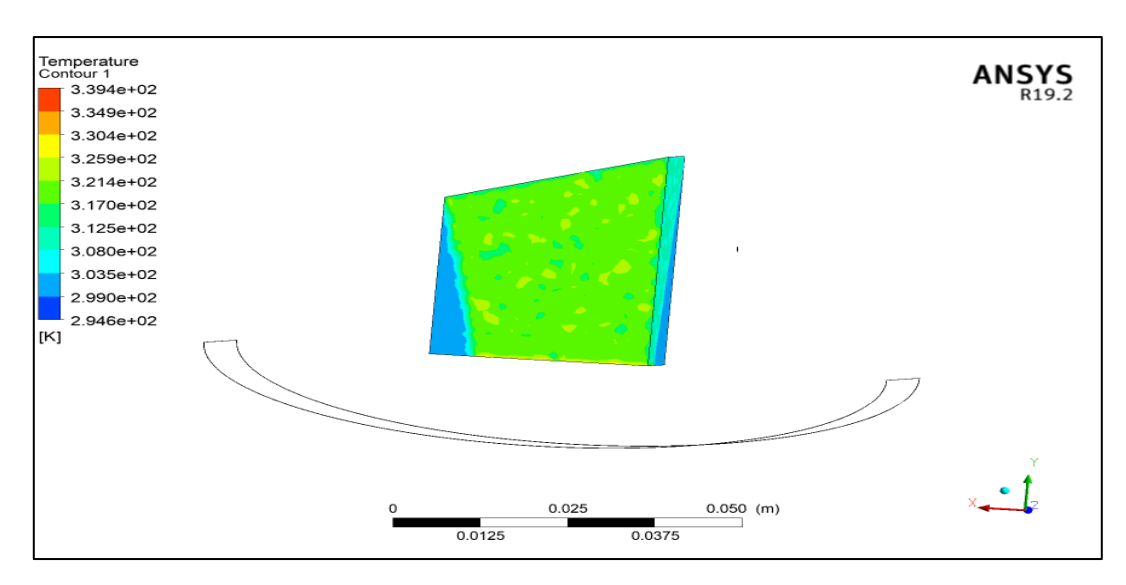


Fig 4.7 Temperature distribution inside the triple basin Side view

Fig. 21 visualizes the gas-phase temperature volume rendering inside the TBSS still. Temperature variation at each stage was calculated inside the still. In the temperature volume rendering, the red colour visualizes the maximum value of the temperature, while the blue colour visualizes the minimum value of the temperature for the system. In TBSS, the temperature is increasing from bottom to top slowly. Basins are attaining max. temperature at the lowermost because of the mesh orientation towards solar incident rays, which were concentrated by the parabolic concentrator.

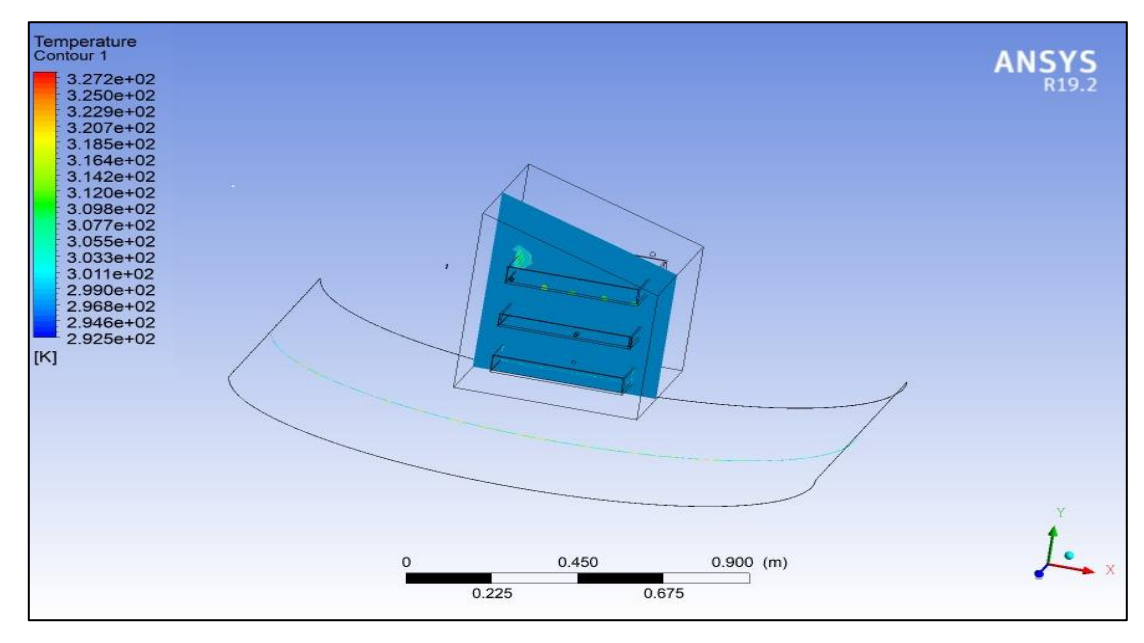


Fig 4.8 Temperature distribution inside pipe flow

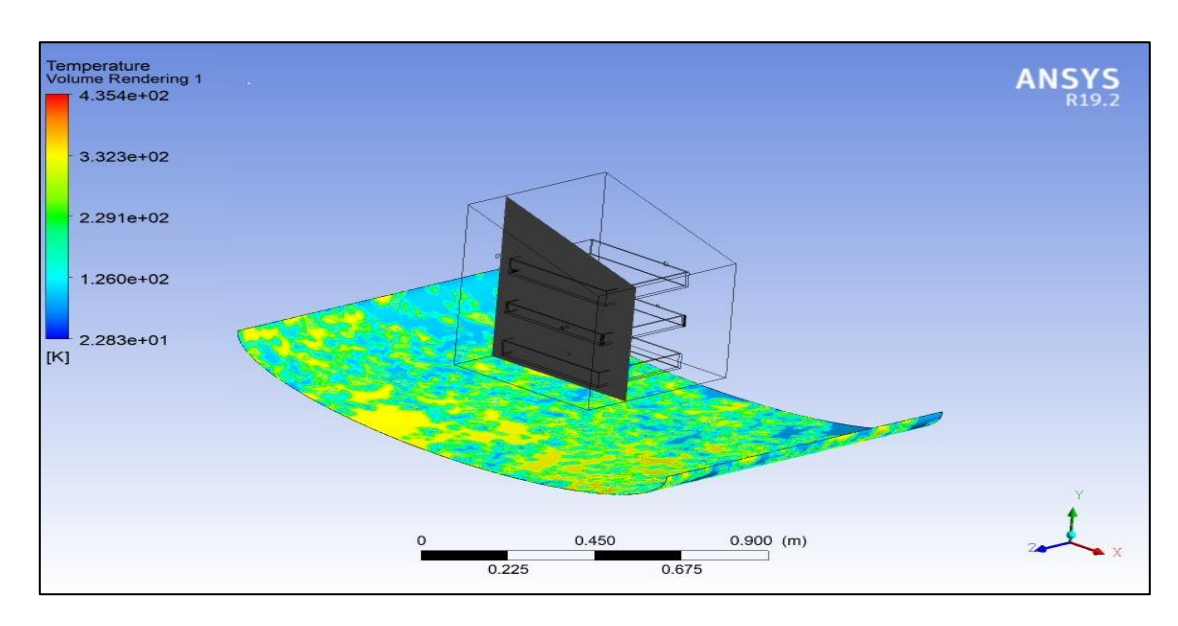


Fig 4.9 Temperature distribution over the surface of parabolic concentrator

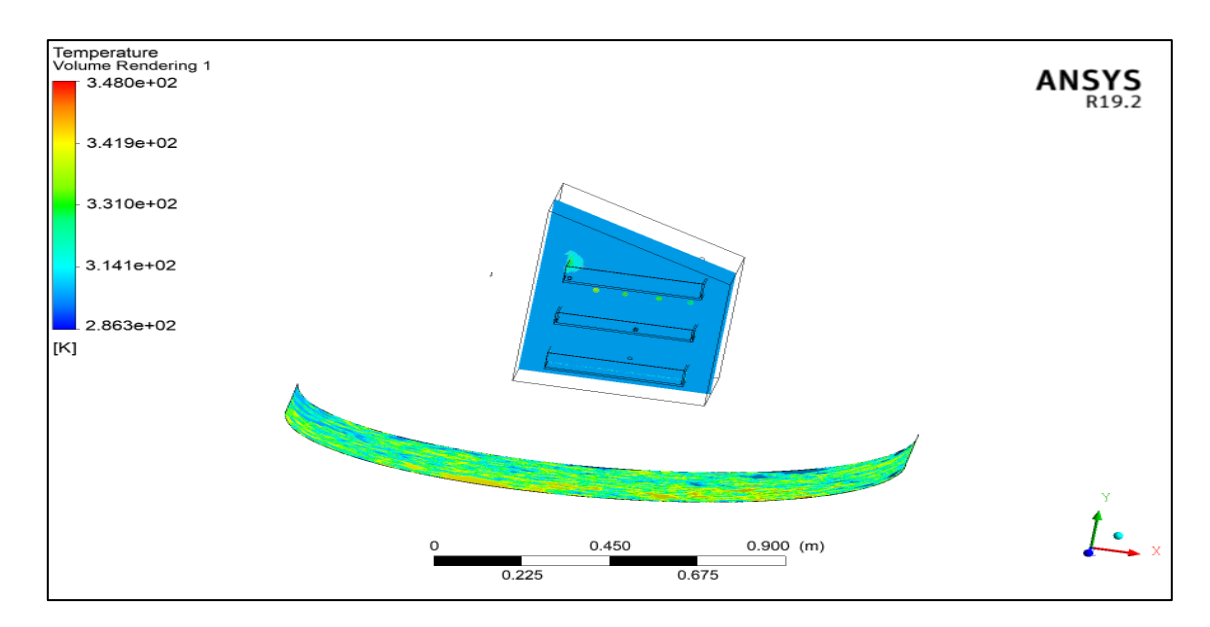


Fig 4.10 Temperature distribution over the surface of parabolic concentrator and pipe flow: combined system

4.3. Temperature Variation with Time:

Figure 25 shows the temperature variation of the Lower Basin of TBSS concerning the time. The temperature of the still is calculated for the entire day. From the simulation result, it was predicted the maximum temperature was obtained at 13:00 hr. i.e., 351.5 K

(78.35 °C) and while the minimum temperature is obtained in the morning during sunrise and sunset i.e., 304.25 K (31.1 °C), which is the very low temperature to convert the water into vapor. The red line in the graph shows the temperature, while the blue line shows time on the streamline. From the graph of a triple basin solar still, it is predicted that there is no time when the temperature inside the TBSS still is constant (Fig.25). From the graph of TBSS still, it is predicted that temperature is almost constant from 12:00 to 12:30 hr. Then, it increases, and at 13:00 hr. it attains maximum temperature. Again, from 14:00 to 14:15 hr., the temperature is almost constant, and it decreases.

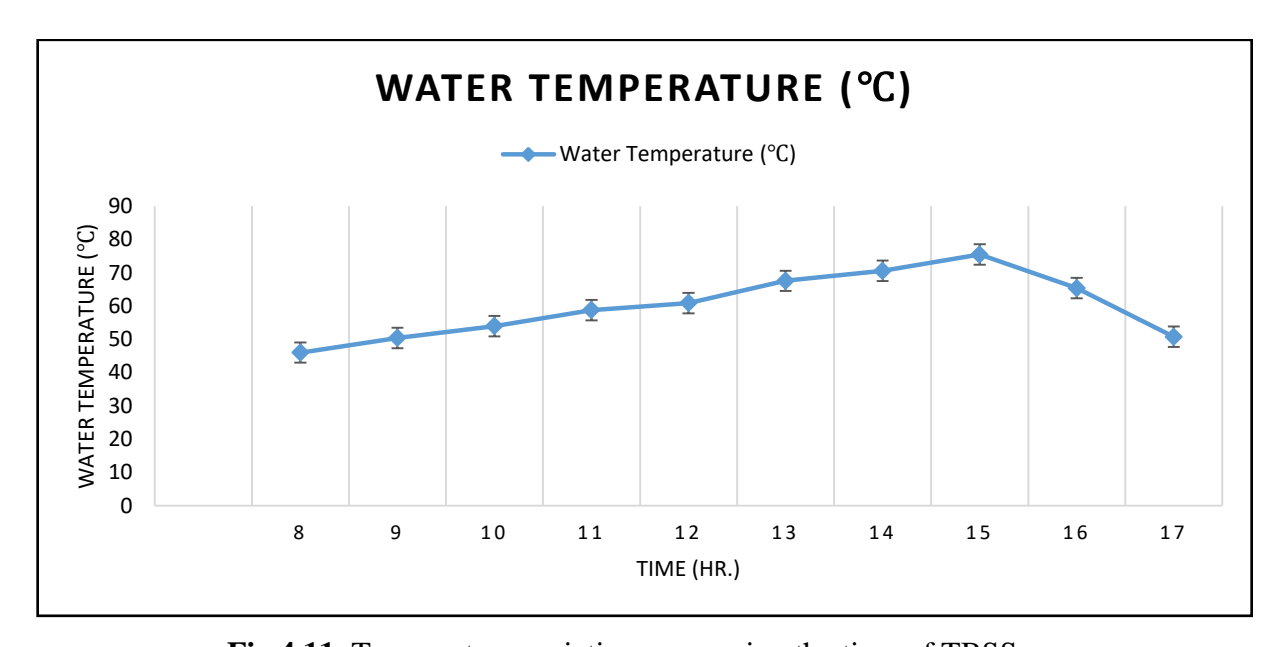


Fig 4.11 Temperature variation concerning the time of TBSS.

4.4 Water Volume Fraction:

The volume fraction of the water contour having the side view of the system is visualized in Figure 26 in which blue color is allowed to visible less volume fraction of water, while red color shows more water vol. fraction. The water volume fraction is increasing from top to bottom inside the still and it is observed maximum volume fraction is near the absorber surface of the bottom basin, i.e 4.15831×10^{-1} and minimum 4.3543×10^{-2} .

Cooled water on the glass is visualized in Figure 27. It is observed that the volume fraction of droplets on the inside of the glass surface in contrast to its surface is less. Water volume

fraction contours having the glass surface view of the system are shown in Figure 27 in which the blue color is visualizing a reduced value of the vol. fraction of water whereas the red color is visualizing more vol. fraction of water. The volume fraction of droplets is increasing downward on the glass. The maximum value of the vol. fraction of water on the glass is 2.911×10^{-1} .

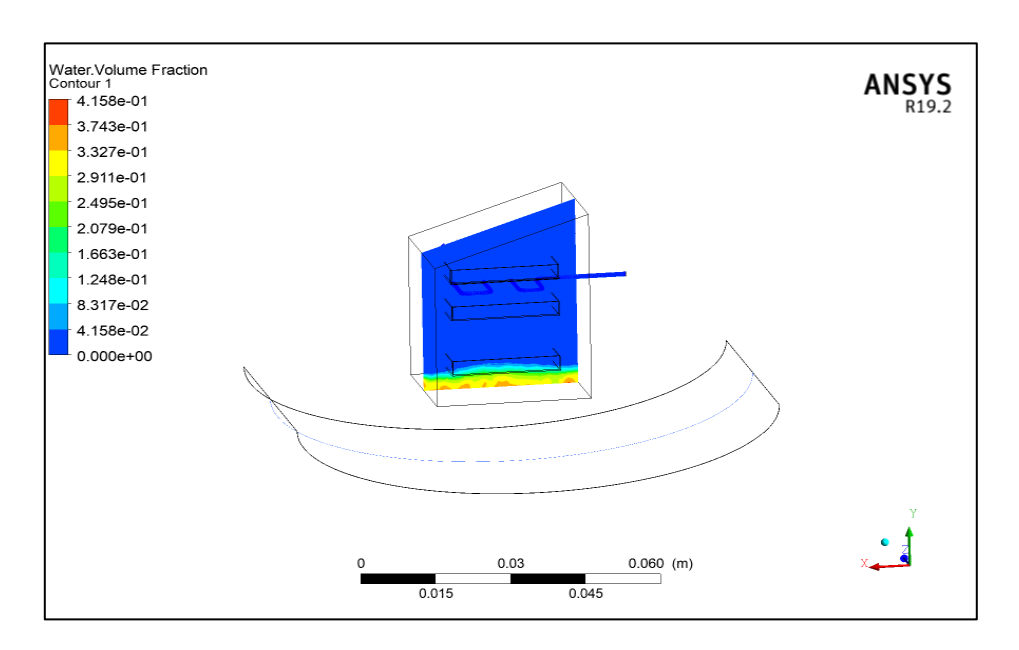


Fig 4.12: - Water vol. fraction contour inside the glass of TBSS

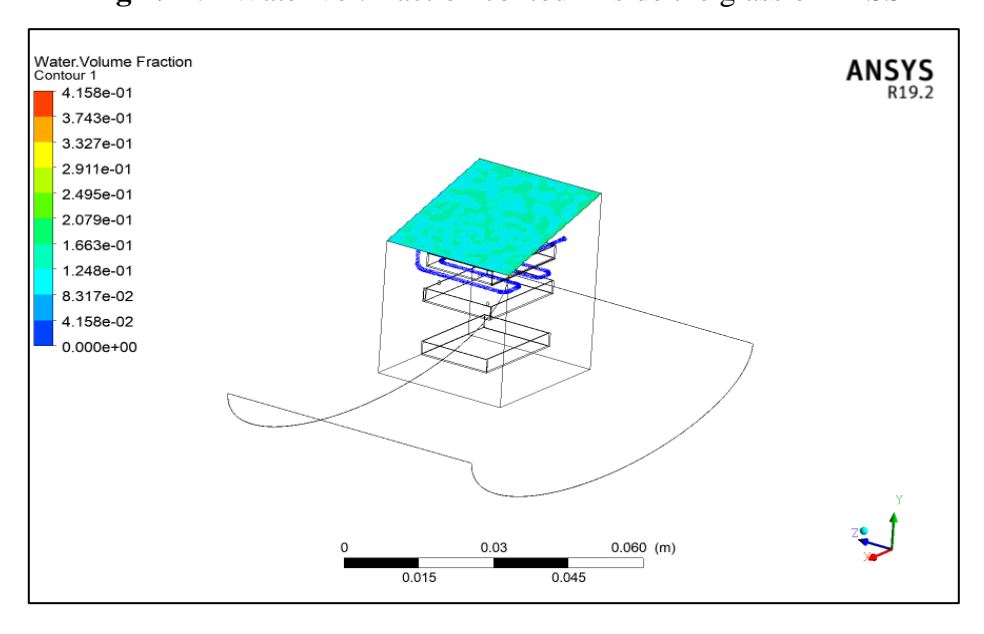


Fig 4.13: - Water vol. fraction contour on the glass of TBSS.

Figure 28 visualizes the volume fraction of water of TBSS still concerning the time. The water volume fraction of the TBSS still is calculated for the entire day. The simulation result predicted the maximum water volume fraction was obtained at 13:00 hr. i.e. 0.999998. The red line in the figure visualizes the vapor volume fraction, while the blue line visualizes time on the streamline. As seen increment in the temperature, the volume fraction of vapors rises remarkably and air lessens remarkably.

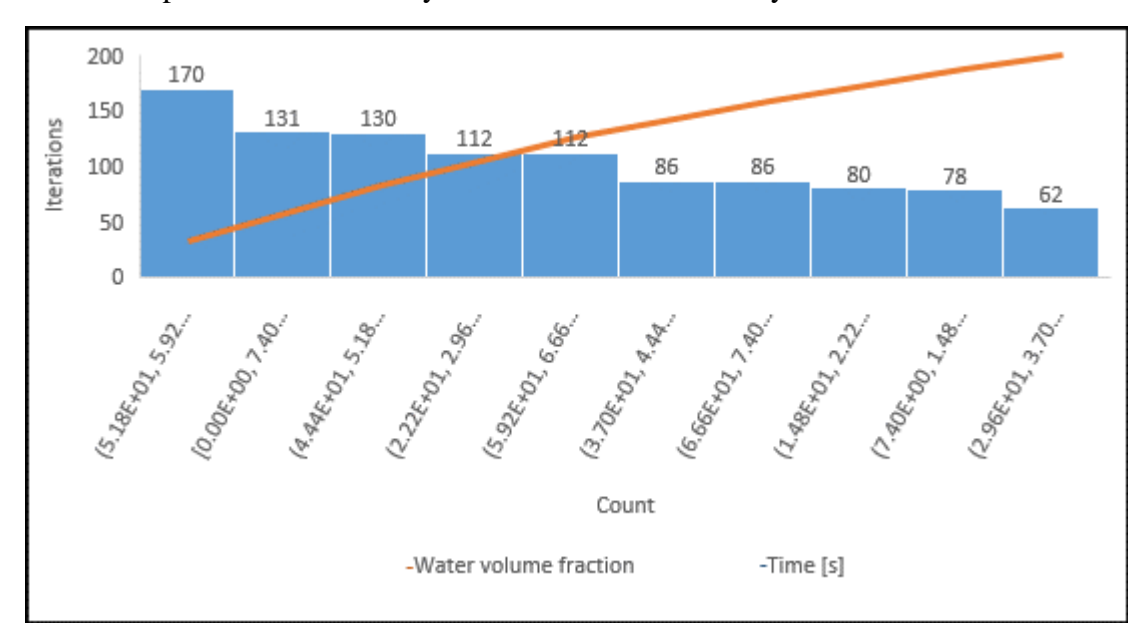


Fig 4.14 Water volume fraction concerning the time of TBSS still.

Volume fraction contours of the vapor having the side view of the system and glass view are visualized in Figures 29 and 30 in which blue color shows less volume fraction of vapor, while red color visualizes more volume fraction of vapor. The volume fraction of vapor decreases from top to bottom inside the still whereas, on glass, the vapor volume fraction is increasing downward of glass. It is observed maximum volume fraction of vapor is 0.6794 and a minimum of 0.06715.

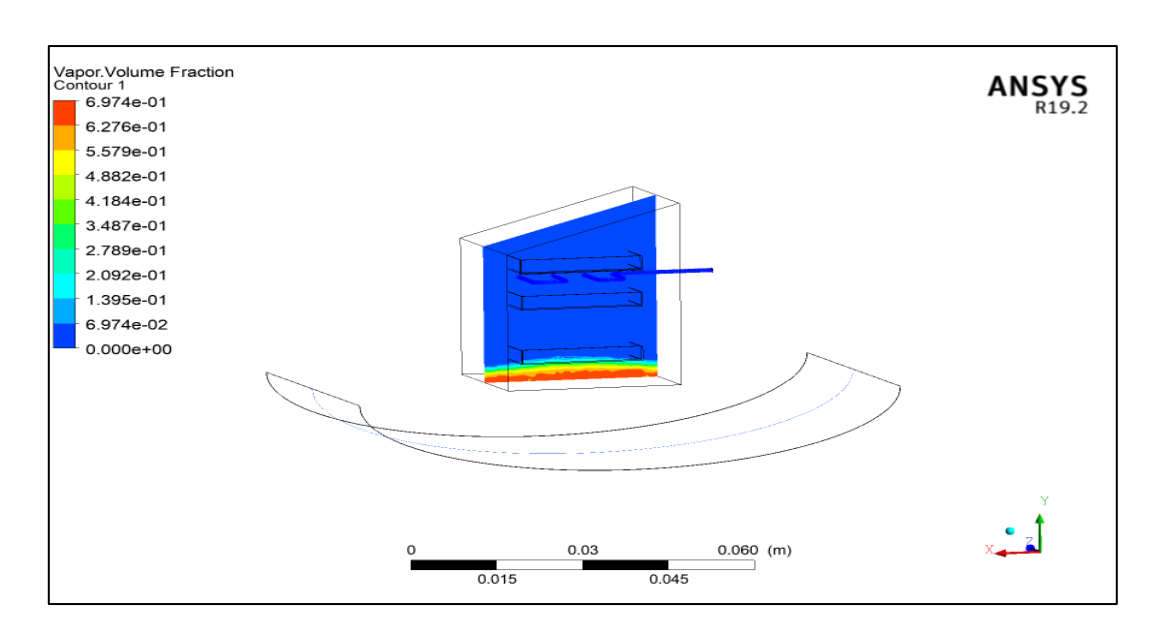


Fig 4.15: Vapour vol. fraction contour on the glass of TBSS

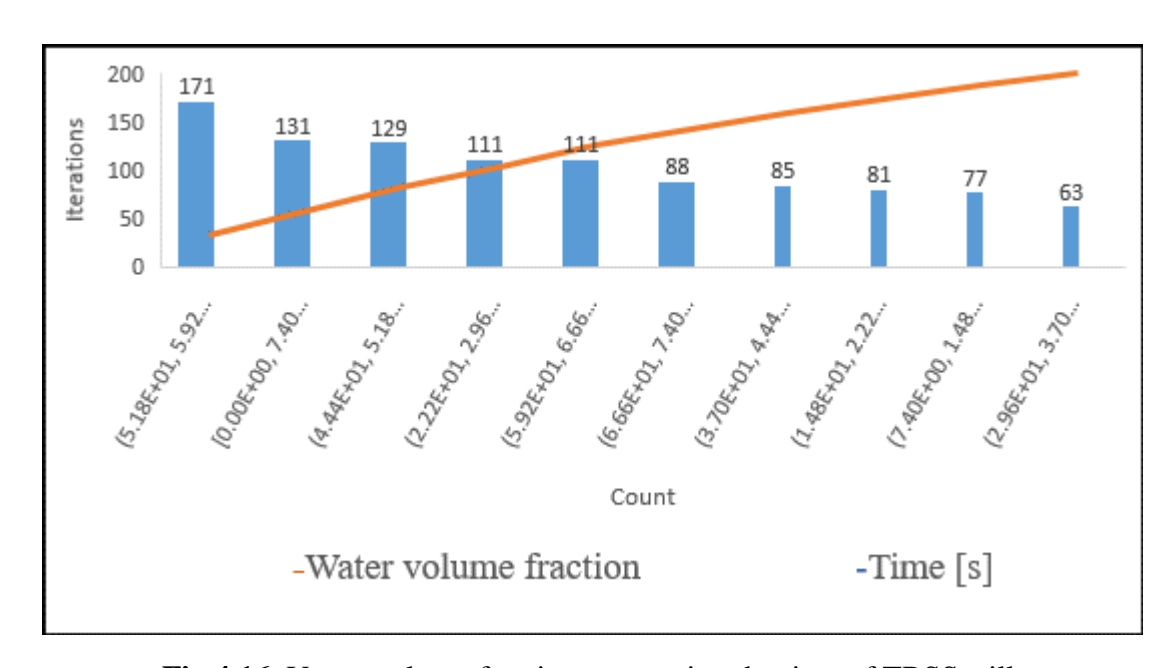


Fig 4.16 Vapor volume fraction concerning the time of TBSS still.

Figure 30 visualizes the vapor volume fraction of TBSS still concerning the time. The vapor volume fraction of the TBSS still is calculated for the entire day. The simulation result predicted the maximum vapor volume fraction was obtained at 13:00 hr. i.e. 0.999998. The red line in Figure 30 shows the vapor volume fraction, while the blue line

shows time on the streamline. From the graph of a still, the conversion of water into vapor increases as time increases. It results in more conversion of water into vapor at 13:00 because of higher solar flux and after time increases, vapor conversion decreases.

4.5 Pressure Variation:

Fig 32 shows the gas-phase pressure-volume rendering inside the TBSS still. Pressure variation at each stage was calculated inside the still. In the pressure-volume rendering, the red color shows max. pressure, while the blue color shows min. pressure for TBSS still. The pressure inside the still, firstly, increases, then decreases and again increases from top to bottom. The maximum pressure is calculated at the top while the minimum temperature is calculated at some height from the absorber. The minimum pressure inside the still is just above the atmospheric pressure. Pressure volume rendering shows the pressure near edges of the walls has the maximum value at glass surface material is 3.775 Pa while remaining free space inside the system has pressure as the minimum of -1.396 Pa.

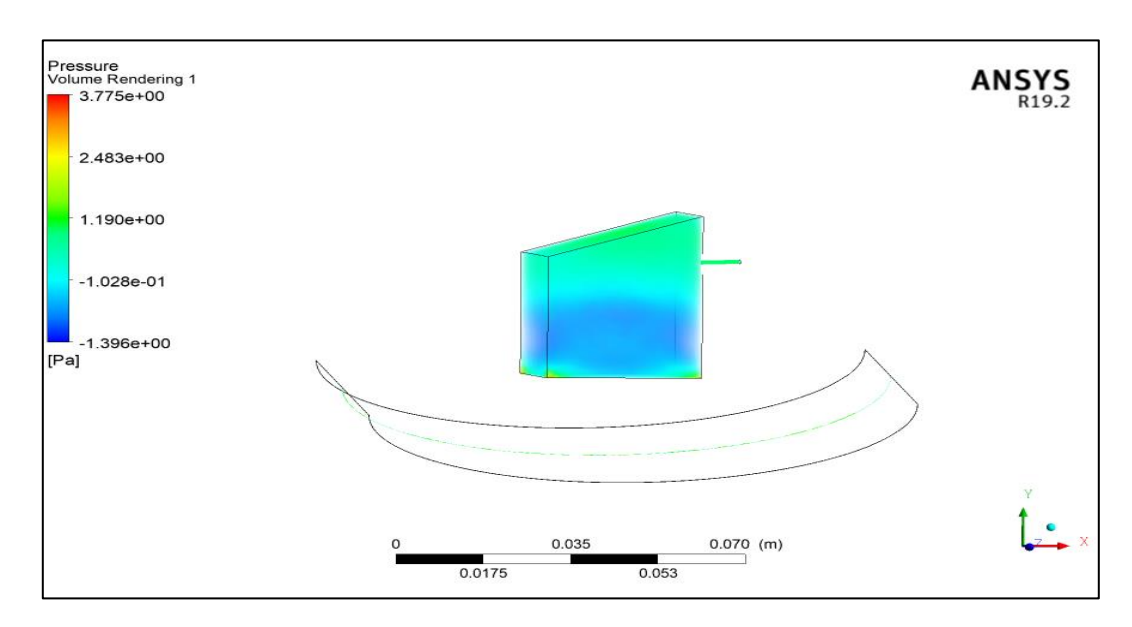


Fig 4.17. Pressure volume rendering inside the TBSS still.

Figure 33 visualizes the pressure variation of TBSS still concerning the time. The pressure of the still is calculated for the entire day. The simulation result predicted the maximum pressure was obtained at 13:00 hr. i.e. 3.775 Pa. The red line in the graph

shows the pressure variation while the blue line shows time on the streamline. With increase time, the pressure of the mixture changes slightly and maximum pressure occurred near opaque material.

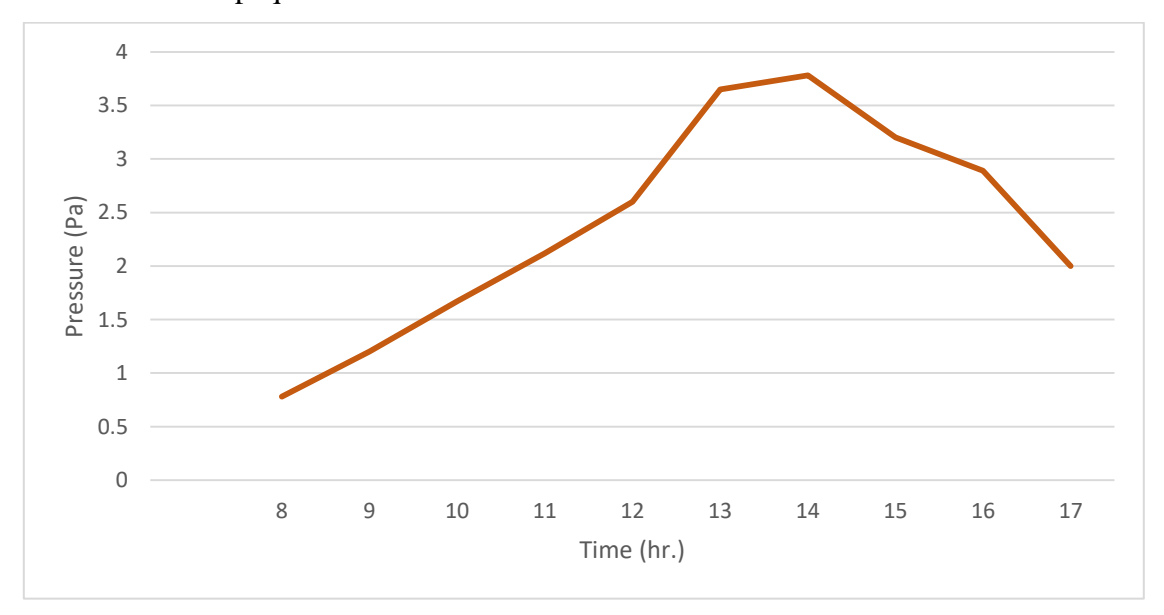


Fig 4.18. Pressure variation concerning time inside TBSS.

4.6 Velocity Distribution:

Figure 34 shows the velocity volume rendering of the mixture inside the TBSS still. The minimum velocity of the mixture is near-transparent material which is zero while the highest value of the velocity is near opaque material i.e. 0.09729ms^{-1} .

More velocity shows more circulation of mixture particles inside the still, i.e., converting water into vapor and moving upward to produce potable water.

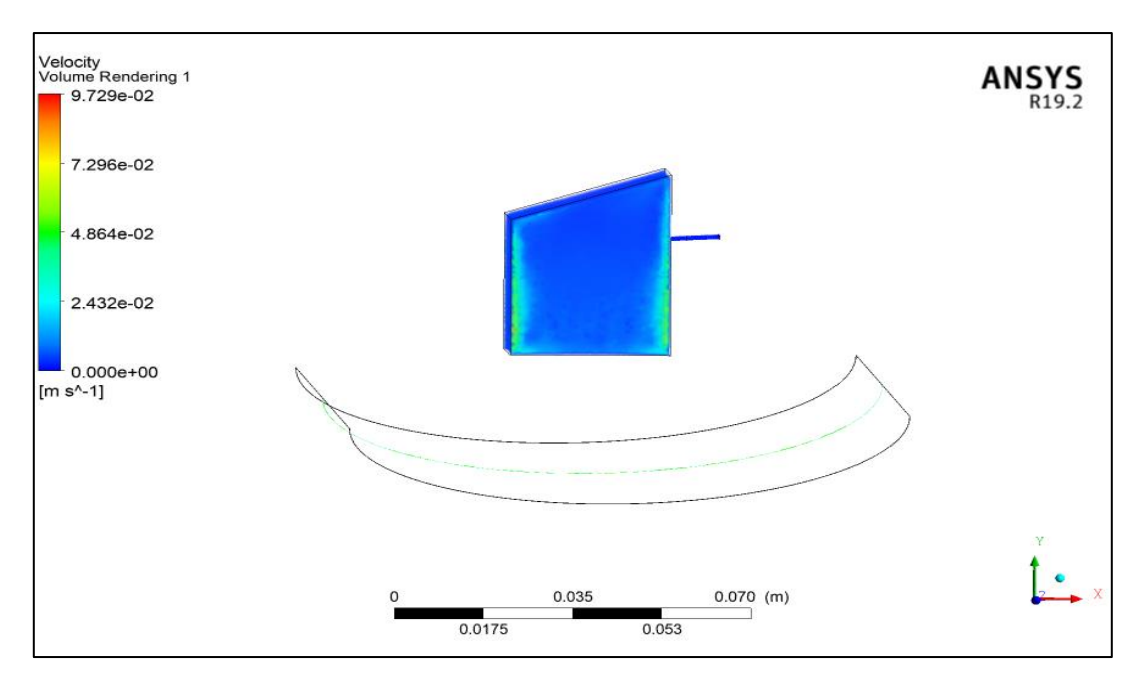


Fig 4.19. Velocity volume rendering inside the TBSS still.

4.7 Mass Flow Rates:

The mass flow rate shows that the mass flow rate is finer inside TBSS still than conventional solar still. The maximum mass flow in TBSS is $4.956e^{-6}~kgs^{-1}m^{-2}$ while, minimum mass flow is $-4.905e^{-6}~kgs^{-1}m^{-2}$.

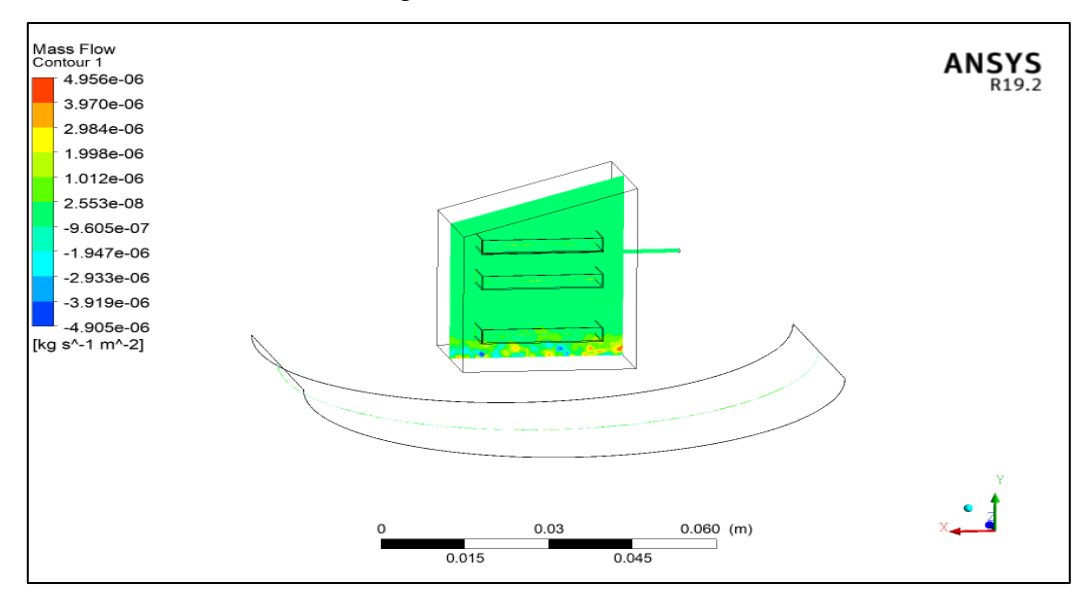


Fig 4.20. Mass flow contour inside the TBSS still.

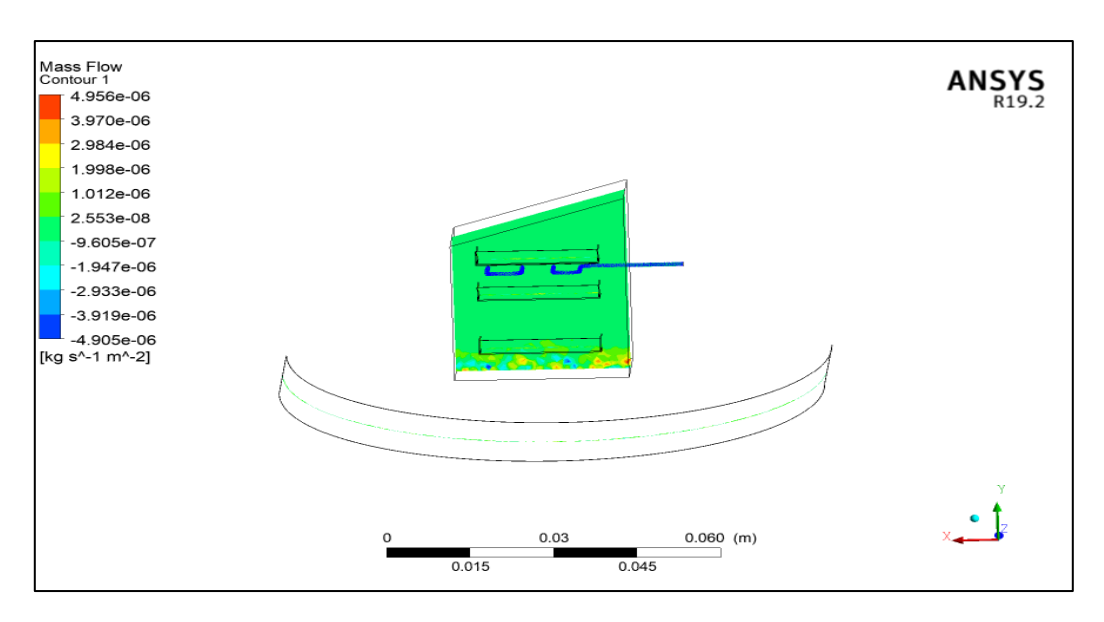


Fig 4.21 Mass flow contour inside the TBSS still.

4.8 Static Enthalpy:

Figure 37 shows the static enthalpy inside the TBSS still. In static enthalpy volume rendering, the red color visualizes the maximum value of static enthalpy while the blue color visualizes the minimum value of static enthalpy inside the TBSS still. Inside the still, different colors are distributed to calculate static enthalpy at each stage. The minimum static enthalpy of the mixture is near-transparent material, which is -1.591e+07 Jkg⁻¹ while maximum static enthalpy is near opaque material i.e. 6.380e+3 Jkg⁻¹. The negative value of static enthalpy means energy is absorbed by water to convert into vapor. In TBSS still, the static enthalpy is increasing from bottom to top rapidly, whereas, in conventional still, the temperature is increasing slowly from bottom to top. Still is attaining maximum static enthalpy at the top because of mesh orientation towards solar incident rays.

The comparison of both TBSS stills and conventional still shows static enthalpy absorbed by TBSS still is better contrast to single slope SS, which affects the production of potable water. More absorption of enthalpy from sunlight shows more conversion of water molecules into vapor, at 13:10 hr maximum enthalpy absorbed by TBSS slope. This difference is because of mesh orientation difference and also depends on glass size.

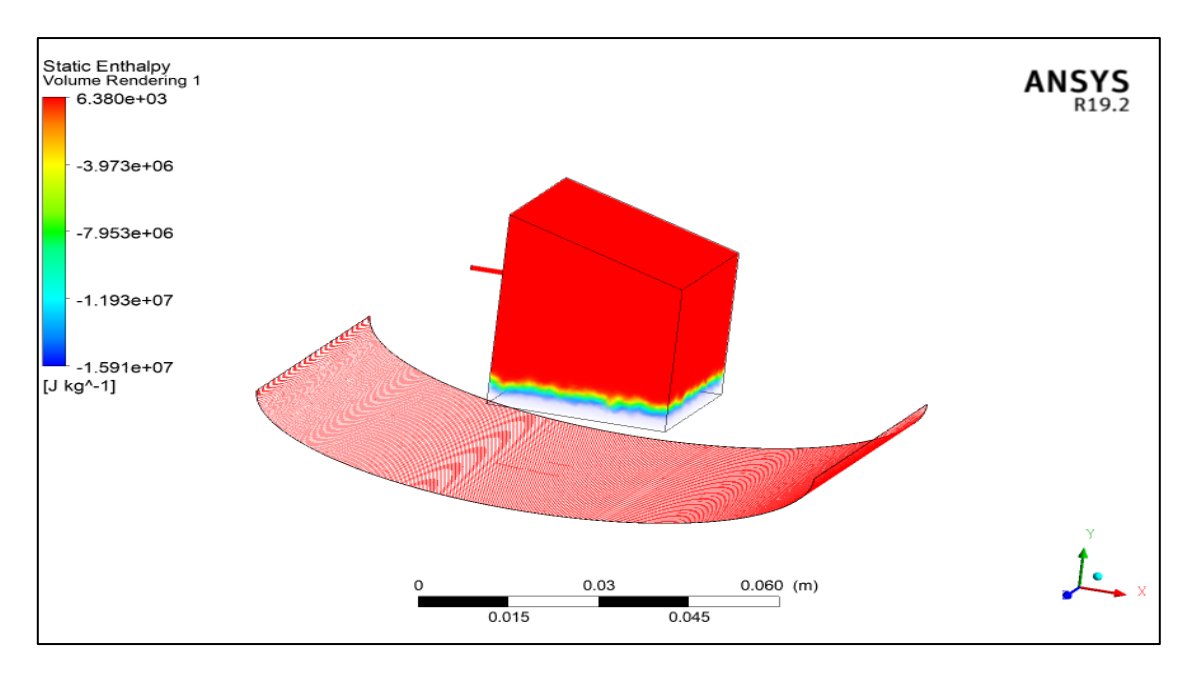


Fig 4.22 Static enthalpy volume rendering inside the TBSS still.

4.9 Absorption Coefficient:

The absorption coefficient relates to the intensity attenuation of the light passing through a material. Figure 34 shows the absorption coefficient volume rendering in which blue color visualizes the lowest value and red color visualizes the highest value of the absorption coefficient. Inside the TBSS still, the red color is more than other colors, which means higher solar energy is taken up using the glass and then transmitted through the glass into the still. The maximum value of the absorption coeff. is $3.842e^{-1}$ m⁻¹ at the base of TBSS while the min. value of the absorption coeff. is $1.000e^{-2}$ m⁻¹ above some height from the base of the still. The min. value of the absorption coeff. on glass is at both upward corners and in the middle part and downward corners of the glass, the absorption coefficient is higher.

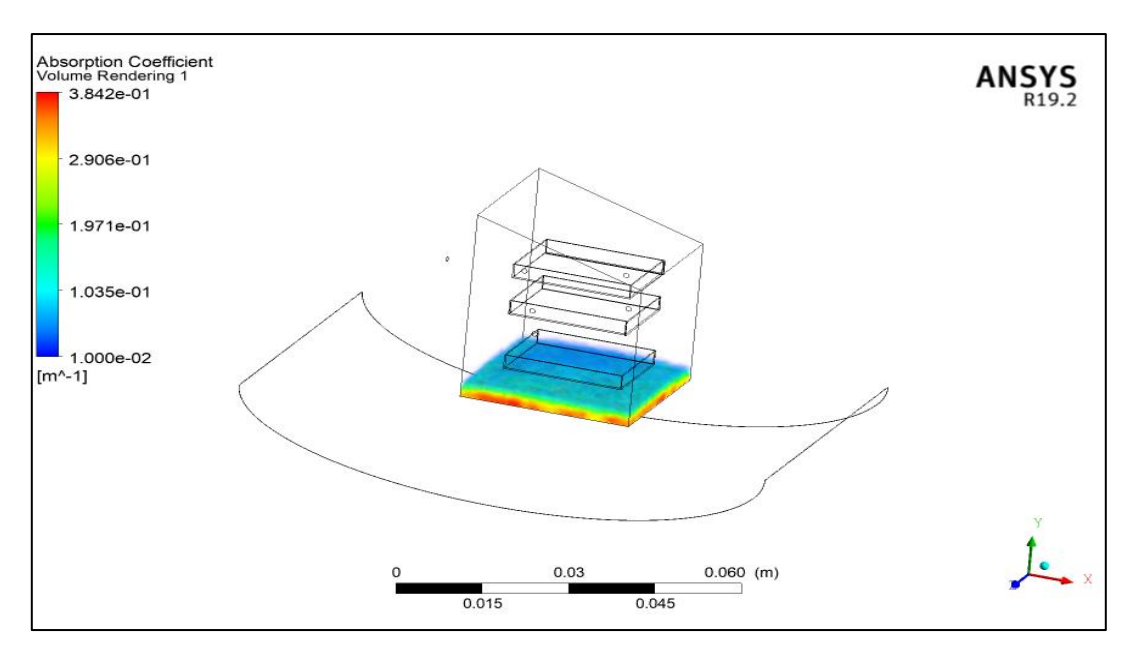


Fig 4.23. Absorption coefficient volume rendering inside the TBSS still.

In comparing the absorption coefficient of both conventional and TBSS stills, it has been noticed about the absorption coefficient of the TBSS system is more compared to conventional still because of the presence of the parabolic concentrator in the present system. Concentrated rays absorb solar energy is higher in contrast with solar still. From the temperature distribution result, it was calculated that TBSS still has higher temperature in contrast with the current system, but the pressure and heat absorption are higher of single slope SS, which affects potable water.

4.10 Turbulence Kinetic Energy:

Turbulence kinetic energy is the kinetic energy contained in unit mass in turbulent flow associated with eddies. It is characterized by measuring V_{rms} (root mean square velocity) fluctuations. Figure 39 shows the turbulence kinetic energy of the mixture inside the TBSS still. The red color in legend shows maximum turbulence kinetic energy while the blue color shows minimum turbulence kinetic energy. Figure 39 depicts that the TBSS system contains turbulence kinetic values inside the casing as the maximum amplitude of 0.9998 m^2s^{-2} and the minimum value as $3.536e^{-3}$. The energy associated with eddies forms a platform for vigorous mixing of fluids and thus energy exchange rate increases which in turn favors evaporation-condensation processes. As the size of the system is complex and

big, it does not have its extreme values but significant enough to encourage the yield of the system.

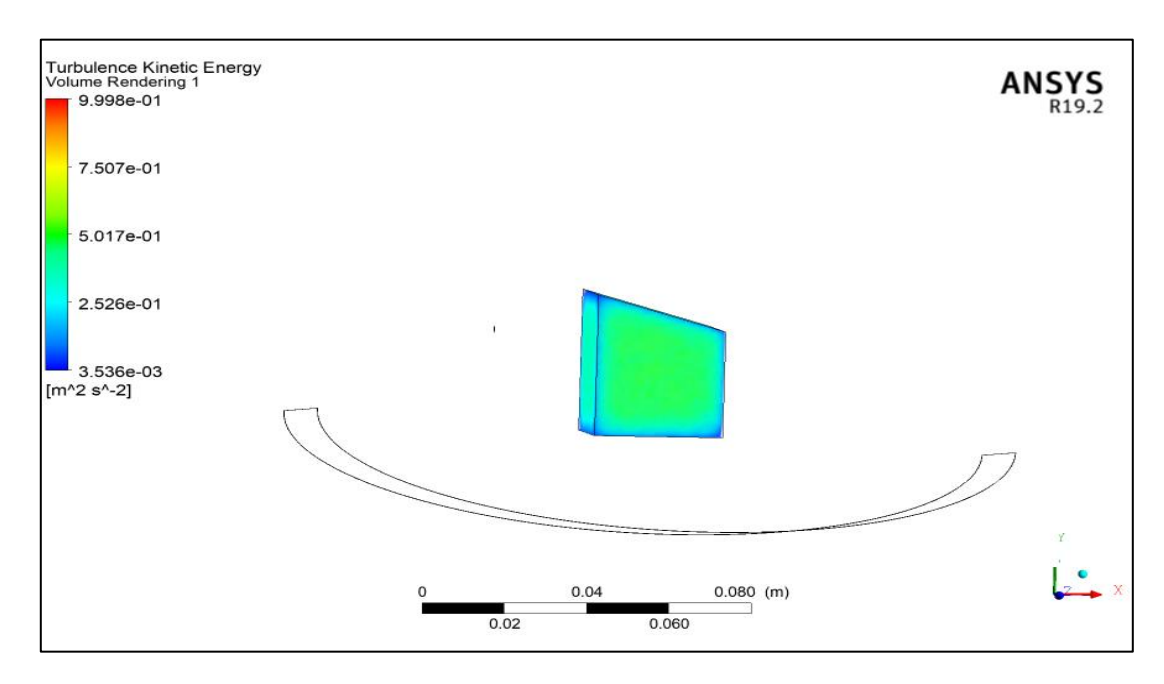


Fig 4.24 Turbulence kinetic energy rendering inside the TBSS still.

4.11 Eddy Viscosity:

Figure 40 shows the eddy viscosity of the mixture inside the TBSS still. The red color in legend shows maximum eddy viscosity while the blue color shows minimum eddy viscosity. The maximum eddy viscosity in TBSS still is 2.347 Pa s and the minimum eddy viscosity is 1.428e⁻⁴ Pa s. Most of the basin areas have lower values of eddy viscosity. The lower basin surface and base of the TBSS contain maximum amplitudes of eddy viscosity.

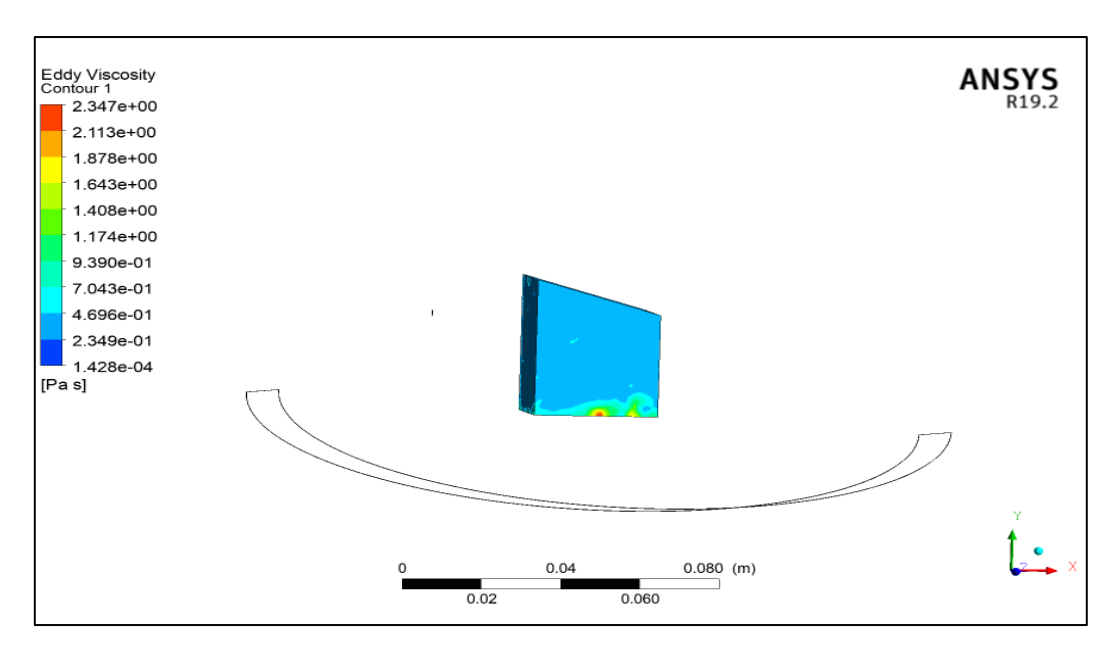


Fig 4.25 Eddy viscosity volume rendering inside the TBSS still.

Eddy viscosity is a proportionality factor that describes turbulent transfer energy in the form of moving eddies. Higher eddy viscosity is calculated inside the basins of TBSS single slope. Hence, turbulence is higher in single slope due to which mixture circulates more inside single slope than TBSS because of the size of the system and particles of the mixture strike on the walls, which results in pressure increase inside the single slope solar still.

4.12 Solar Heat Flux:

Figure 41 shows the solar heat flux variation of TBSS still concerning the time. The solar heat flux of the TBSS still is calculated for the entire day. The red line in Figure 41 shows solar heat flux while the blue line shows streamline time. From the simulation result, it was predicted the solar heat flux first raises with time after sunrise and then starts to lessen as time increases afternoon. The maximum solar flux was obtained at 13:00 hr. due to which still gains high temperature while the minimum solar heat flux was obtained in the morning during sunrise and sunset which produce low temperatures to convert the water into vapor. Solar heat flux again slightly increases after 14:30 hr. and then again decreases. After 15:15 hr. solar heat flux increases but not for more time. This process continues until sunset.

From the graph of a TBSS still, it is also predicted that there is no time when the solar heat flux inside the still system is constant.

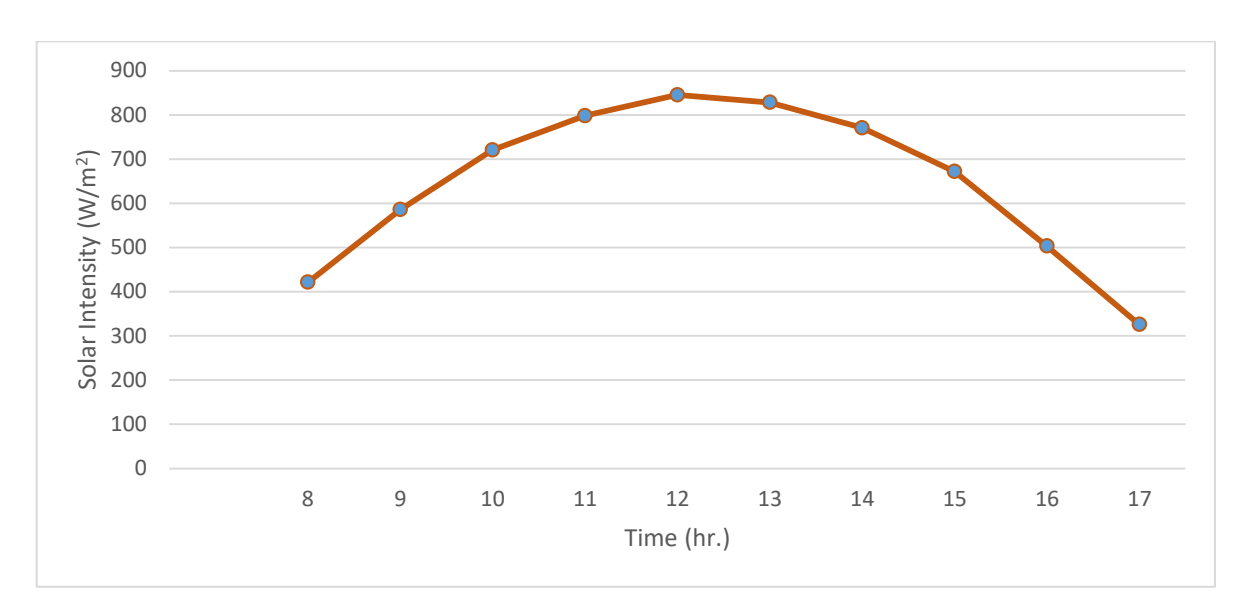


Fig 4.26 Solar heat flux concerning time inside the TBSS still.

4.12 Water Production Rate:

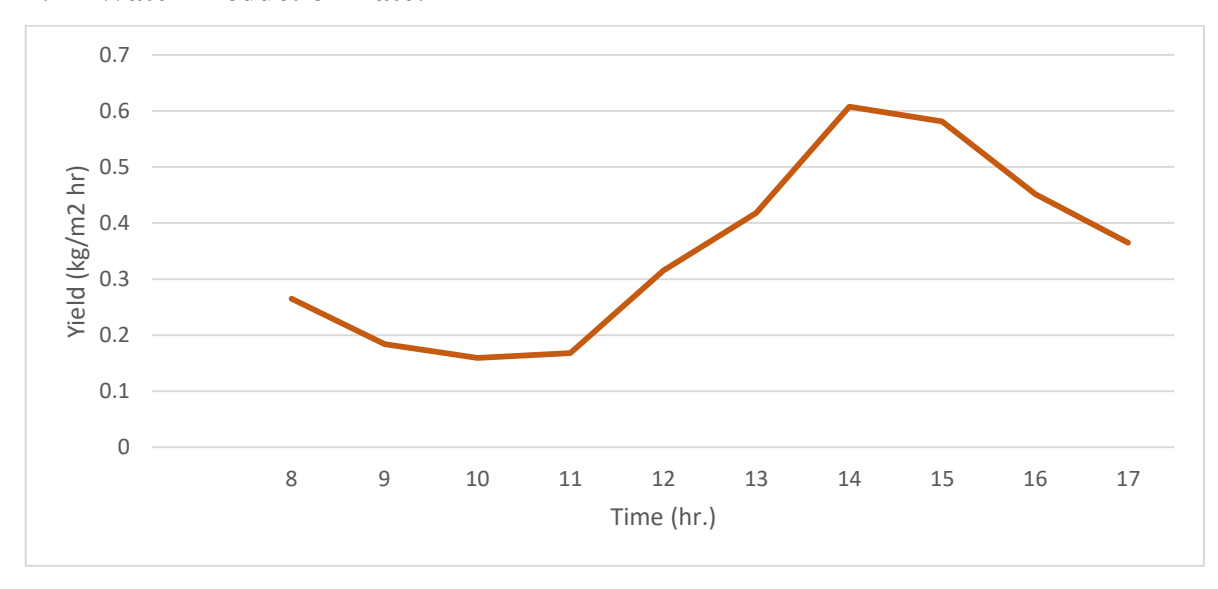


Fig 4.27 Water production rate concerning time inside the TBSS still with the parabolic collector.

Figure 41 visualizes the graph of the water production rate concerning the time. The simulation still runs at 6.30 hr. time. In this figure, it is noted that as the action starts at 8:00 hr., time passes and water starts to warm up due to solar radiation absorbed by water. Moderately still space heats up with water vapor and the freshwater production rate raises till 13:30 hr and after when solar radiation decreases water moves downward slowly.

It was found out that this system with charcoal filled fins and parabolic concentrator along with cooling water arrangement at the top attains water production yield at a rate of 16.78 kgm⁻²day⁻¹.

Water production of still, it was observed that water production of TBSS still with single slope equipped with parabolic concentrator is more compared to conventional solar still. Some terms affect water production, such as temperature, mass flow, pressure, solar heat flux, absorption coefficient, and many other factors. These all terms are checked in the simulation of still and observed that a TBSS is more capable of producing freshwater in rural and urban areas.

4.13 Percentage Deviation

Parameters		Theoretical	Experimental	% Deviation
		Readings	Readings	
Temperature with time	variation	78.35 °C	85 °C	8.48%
Productivity		16.78 Kgm ⁻² day ⁻¹	16.94 Kgm ⁻² day ⁻¹	0.95%

There is significant deviation from the experimental and theoretical readings due to the following reasons:

Parabolic concentrator reflector sheets material and arrangement. Weather conditions (heat flux) in real world are different as in case of simulation. Insulation and material, cooling water flow rate and thickness variation. Impurities in saline water deviates results as simulated.

CHAPTER 5

CONCLUSION

The major motive of the research is to make a computational fluid dynamics model of TBSS system with parabolic concentrator. A three-dimensional model of the setup is developed using computational fluid dynamics. In the setup, evaporation & condensation processes take place. Models were organized for water-mix (air and water vapour) systems with ANSYS FLUENT V19.2 software. The computational fluid dynamics simulation was conducted for transient conditions using these models. The simulation data of the system is obtained in 12 hours with 200 steps of 15 minutes period. In the system, water absorbs solar radiation and evaporates the vapour which condenses on the glass's inner surface.

The concluding remarks of the study are:

- The maximum temperature of air and water-vapor mix inside the system is 351.5
 K and the minimum temperature is 304.25 K
- It was found that the temperature continuously varies as time pasts. It reaches a peak at the noon and decreases after that. Provision of heat storage material inside the fins steadies the fluctuation over the increased interval of time.
- Parabolic concentrator causes the maximum sunlight to concentrate on the surface
 of the glass basin and that trapped radiation increases the temperature of the
 system. Peak temperature of the system raises to 78.35 °C for the current system.
- The maximum water volume fraction is near absorber i.e 0.4158 and a minimum 4.158e⁻² in TBSS.
- The maximum volume fraction of vapour is 0.6794 and a minimum of 0.06715 in TBSS. Maximum vapour concentration is found at the base surface of the basin due to direct collective radiation incidented over this susrface which causes rapid evaporation.
- Pressure volume rendering shows the pressure near edges of the walls has maximum value at glass surface material is 3.775 Pa while remaining free space inside the system has pressure as minimum of -1.396 Pa.

- The maximum mass flow in TBSS is $4.956e^{-6} \text{ kgs}^{-1}\text{m}^{-2}$ while, minimum mass flow is $-4.905e^{-6} \text{ kgs}^{-1}\text{m}^{-2}$.
- The maximum water production rate in a TBSS is 16.78 kg m⁻²day⁻¹ when the system is equipped with heat storage material, concentrator, cooling water arrangement, and proper insulation.
- The maximum temperature of the system with triangular fins is more than maximum temperature with cylindrical fins. Maximum temperature with triangular fins is 73.112°C and with cylindrical fins is 66.09°C.
- The temperature distribution is concentrated at the edge of the triangular fin but will have symmetrical distribution in the case of cylindrical fins.
- Percentage deviation is 8.48% and 0.95% for peak temperature distribution and productivity respectively.

It was predicted that computational fluid dynamics results visualize that computational fluid dynamics are strong equipment for the designing process, variable investigation, and can be used for removing difficulties during geometry creation of solar still construction. In the future, further work can be done by modifying different design parameters and orientation of solar still.

REFERENCES

- https://water.org/our-impact/water-crisis/ (24/04/2020, 11:00 am) World Health Organization and UNICEF Joint Monitoring Programme. (2017). Progress on Drinking Water and Sanitation, 2017 Update and MDG Assessment.
- 2) https://en.wikipedia.org/wiki/Water_distribution_on_Earth(24/04/2020, 10:55am)
- 3) CBHI & Ministry of Health
- 4) M.K. Phadatare, S.K. Verma, Influence of water depth on internal heat and mass transfer in a plastic solar still plastic solar still, Desalination 217 (2007).
- 5) T. Elango, K.K. Murugavel, The effect of the water depth on the productivity for single and double basin double slope glass solar stills, Desalination 359 (2015).
- 6) Y.A.F. El-Samadony, A.E. Kabeel, Theoretical estimation of the optimum glass cover water film cooling parameters combinations of a stepped solar still, Energy 68 (2014).
- 7) T. Arunkumar, R. Jayaprakash, A. Ahsan, D. Denkenberger, M.S. Okundamiya, Effect of water and air flow on concentric tubular solar water desalting system, Appl. Energy 103 (2013).
- 8) T. Rajaseenivasan, T. Elango, K.K. Murugavel, Comparative study of double basin and single basin solar stills, Desalination 309 (2013).
- 9) T. Rajaseenivasan, K.K. Murugavel, Theoretical and experimental investigation on double basin double slope solar still, Desalination 319 (2013).
- 10) H.N. Panchal, Enhancement of distillate output of double basin solar still with vacuum tubes, J. King Saud Univ. e Eng. Sci. 27 (2015).
- 11) T. Rajaseenivasan, K.K. Murugavel, T. Elango, R.S. Hansen, A review of different methods to enhance the productivity of the multi-effect solar still, Renew. Sustain. Energy Rev. 17 (2013).
- 12) F. Xiong, G. Xie, H. Zheng, Experimental and numerical study on a new multieffect

- solar still with enhanced condensation surface, Energy Convers. Manag. 73 (2013).
- 13) V. Velmurugan, M. Gopalakrishnan, R. Raghu, K. Srithar, Single basin solar still with fin for enhancing productivity, Energy Convers. Manag. 49 (2008).
- 14) A.A. El-Sebaii, M.R.I. Ramadan, S. Aboul-Enein, M. El-Naggar, Effect of fin configuration parameters on single basin solar still performance, Desalination 365 (2015).
- 15) K.K. Murugavel, K. Srithar, Performance study on basin type double slope solar still with different wick materials and minimum mass of water, Renew. Energy 36 (2011).
- 16) K.K. Murugavel, S. Sivakumar, J.R. Ahamed, Chockalingam KnKSK, K. Srithar, Single basin double slope solar still with minimum basin depth and energy storing materials, Appl. Energy 87 (2010).
- 17) Z.M. Omara, M.A. Eltawil, Hybrid of solar dish concentrator, new boiler and simple solar collector for brackish water desalination, Desalination 326 (2013).
- 18) J.T. Mahdi, B.E. Smith, Solar distillation of water using a v-trough solar concentrator with a wick-type solar still, Renew. Energy 5 (1) (1994).
- 19) T. Arunkumar, D. Denkenberger, A. Ahsan, R. Jayaprakash, The augmentation of distillate yield by using concentrator coupled solar still with phase change material, Desalination 314 (2013).
- 20) T. Rajaseenivasan, K.K. Murugavel, T. Elango, Performance and exergy analysis of a double-basin solar still with different materials in basin, Desalination Water Treat. 55 (7) (2015).
- 21) Z.M. Omara, M.A. Eltawil, E.A. ElNashar, A new hybrid desalination system using wicks/solar still and evacuated solar water heater, Desalination 325 (2013).
- 22) T. Rajaseenivasan, P.N. Raja, K. Srithar, An experimental investigation on a solar still with an integrated flat plate collector, Desalination 347 (2014).

- 23) R. Kannan, C. Selvaganesan, M. Vignesh, B.R. Babu, M. Fuentes, M. Vivar, I. Skryabin, K. Srithar, Solar still with vapour adsorption basin: Performance analysis, Renew. Energy 62 (2014).
- 24) V. Velmurugan, K.J.N. Kumar, T.N. Haq, K. Srithar, Performance analysis in stepped solar still for effluent desalination, Energy 34 (2009).
- 25) H. Nishikawa, T. Tsuchiya, Y. Narasaki, I. Kamiya, H. Sato, Triple effect evacuated solar still system for getting fresh water from seawater, Appl. Therm. Eng. 18 (1998).
- 26) A.A. El-Sebaii, Thermal performance of a triple-basin solar still, Desalination 174 (2005) 23e37.
- 27) Jianyin Xiong, Guo Xie, Hongfei Zheng, Experimental and numerical study on a new multi-effect solar still with enhanced condensation surface, Energy Convers. Manag. 73 (2013) 176e185.
- 28) Mansoor Feilizadeh, M.R. Karimi Estahbanati, Khosrow Jafarpur, Reza Roostaazad, Mehrzad Feilizadeh, Hamed Taghvaei, Year-round outdoor experiments on a multistage active solar still with different numbers of solar collectors, Appl. Energy 152 (2015) 39e46.
- 29) T. Rajaseenivasan, K. Srithar, Performance investigation on solar still with circular and square fins in basin with CO2 mitigation and economic analysis, Desalination 380 (2016) 66e74.
- 30) A.E. Kabeel, A.M. Hamed, S.A. El-Agouz, Cost analysis of different solar still configurations, Energy 35 (2010) 2901e2908.
- 31) Srithar, K., et al. "Stand alone triple basin solar desalination system with cover cooling and parabolic dish concentrator." *Renewable energy* 90 (2016): 157-165.
- 32) https://www.vivintsolar.com/learning-center/how-solar-fits-into-the-world-of-renewable-energy

- 33) Alsaman, A.S., Askalany, A.A., Harby, K. and Ahmed, M.S., 2016. A state of the art of hybrid adsorption desalination–cooling systems. *Renewable and Sustainable Energy Reviews*, 58, pp.692-703
- 34) Water scarcity: India's demand may exceed supply two times by 2030
- 35) http://www.pvcompare.net/news-from-website/101-solar-power-alternatives-omsun-s-newest-technological-move-to-help-sustain-ecological-balance
- 36) Water distribution/https://www.dw.com/en/are-we-running-out-of-fresh-water/a-40241057/>
- 37) Water borne diseaseshttps://argucom.org.in/livpure-vs-kent-water-purifiers/
- 38) Synergy enviro engineers/http://www.synergyenviron.com/tools/solar-irradiance/india/.
- 39) Desalination and water purification technology, Bhabha Atomic research center</h>
 http://barc.gov.in/publications/eb/desalination.pdf>/
- 40) Thole B (2013) Groundwater contamination with fluoride and potential fluoride removal technologies for east and southern Africa
- 41) Q. Chen, M. Kum Ja, Y. Li, K. J. Chua (2017) evaluation of solar-powered sprayassisted low-temperature desalination technology. Applied energy 211:997-1008
- 42) Tan CH, Lefebvre O, Zhang J, Ng HY, Ong SL (2012) Membrane processes for Desalination: Overview.
- 43) Setoodeh N, Rahimi R, Ameri A (2011) Modelling and determination of heat transfer coefficient in-basin solar still. Desalination, 268,103-110.
- 44) Khare V R, Singh P A, Kumar H, Khatri R (2017) modeling and performance enhancement of single slope solar still using computational fluid dynamics. Energy Procedia, 109, 447—455.
- 45) Panchal H.N, Shah P K (2011) Modelling and verification of single slope still using ANSYS-CFX. International Journal of Energy and Environment, 2(6), 985-998.
- 46) Maheswari C.U, Reddy B.V, Sree A.N, Reddy V, Reddy S.P, Prasad R.R, Varma B.H.K (2016) Computational fluid dynamics analysis of single basin double slope solar still. Invention Journal of Research Technology in Engineering & Management, 2, 01-05.
- 47) Fathy M, Hassan H, Ahmed MS (2018) Experimental study on the effect of coupling parabolic trough collector with double slope still on its performance. Sol Energy,163,

54-61.

- 48) Madhlopa A, Johnstone CM (2011) computation of solar radiation distribution in a solar still with internal and external reflectors. Sol Energy, 85(2), 217-233.
- 49) Panchal HN (2010) experimental analysis of different absorber plates on the performance of double slope solar still. Int J of Engineering Science and Technology, 2(11), 6626-6629.
- 50) Tripathi R, Tiwari GN (2005) effect of water depth on internal heat and mass transfer for active solar distillation. Desalination, 173, 187-200.
- 51) Badran O.O (2007) experimental study of the enhancement parameters on a single slope solar still productivity. Desalination, 209, 136-143.
- 52) Singh N (2013) performance analysis of single slope solar stills at different inclination angles: an indoor simulation. Int J Curr Eng Technol, 3(2), 2277-4106.
- 53) Akash BA, Mohsen MS, Osta O, Elayan Y (1998) experimental Evaluation of single basin solar still using different absorbing materials. Renewable energy, 14, 307-310.
- 54) Gokilavani NS, Prabhakaran D, Kannadasan T (2014) Experimental studies and CFD modeling on solar distillation system. Int J Innov Res Sci Eng Technol, 3(9), 15818-15822.
- 55) Singh A, Mittal M.K. (2014) Simulation of single slope solar still at different inclinations using CFD. Int Conf Adv Res Inno,512-519.
- 56) Bhaisare A, Hiwakar A, Sakhare A, Ukey S, Purty S, Wasnik U, P V.K (2019) Brackish Water Distillation System for Gorewada Water Treatment Plant, Nagpur By Using Solar Energy- A Case Study. World Journal of Engineering Research and Technology, 198-215.
- 57) Badusha R, Arjunan T.V (2013) Performance analysis of single slope solar still. international journal of mechanical engineering and robotics research,3(3), 2278-0149.
- 58) Thakur AK, Pathak S.K (2017) Single basin solar still with varying depth of water: optimization by the computational method. Iranian Journal of Energy & Environment, 8(3), 216-223.
- 59) Chinnathambi S, Sridharan M (2014) Performance enhancement study on single basin double slope solar still using flat plate collector. Int J Innov Res Eng Technol, 3(3), 1303-1308.
- 60) Panchal HN, Patel N (2017) ANSYS CFD and experimental comparison of various parameters of a solar still. Int J Ambient Energy,1-7.

- 61) SampathKumar K, Senthilkumar P (2012) utilization of solar water heater in single basin slope still- an experimental study. Desalination, 297, 8-19.
- 62) Tabrizi FF, Sharak AZ (2010) experimental study of integrated basin solar still with a sandy reservoir. Desalination, 253, 195-199.
- 63) Dimri V, Sarkar B, Singh U, Tiwari GN (2008) effect of condensing cover material on the yield of active solar still: an experimental validation. Desalination, 227, 178-189.
- 64) Sharma M, Tiwari AK, Mishra DB (2016) a review on the desalination of water using single slope passive solar still. Int J Develop Research, 11, 10002-10012.
- 65) Chaibi MT (2000) analysis by simulation of a solar still integrated with a greenhouse roof. Desalination, 128, 123-138.
- 66) Ghoneyem A, Ileri A (1997) software to analyze solar stills and an experimental study on the effects of the cover. Desalination, 114, 37-44.
- 67) Mahendren R, Senthilkumar R, Irfan Ali MD (2011) modeling of solar still using granular activated carbon in Matlab. Bonfring Int J Power Sys and Int circuits, 1, 5-10.
- 68) Panchal HN, Doshi M, Chavda P, Goswami R (2011) effect of cow dung cakes inside basin on heat transfer coefficients and productivity of single basin single slope solar still. Int J App Eng Res Dindigul, 1(4), 675-690.
- 69) Shukla M, Ashkedhar RD, Modak JP (2014) an experimental investigation into the performance of GI basin passive solar still using horizontal mesh and vertical mesh. Int J Res in Eng and Technol, 3, 39-63.
- 70) Nayak AK, Dev R (2016) thermal modeling and performance study by modified double slope solar still. Int J Res in Eng and Technol, 5, 19-23.
- 71) Abdallah S, Badran O, Abu- Khadar MM (2008) performance evaluation of the modified design of single slope solar still. Desalination, 219(1-3), 222-230.
- 72) Bellos E, Tzivanidis C (2018) Analytical Expression of Parabolic Trough Solar Collector Performance. *Designs*, 2(1):9
- 73) Khare V R, Singh P A, Kumar H, Khatri R (2017), "Modelling and performance enhancement of single slope solar still using computational fluid dynamics", *Energy Procedia*, **109**, 447—455 doi: 10.1016/j.egypro.2017.03.064
- 74) Kumar, Rohit, and Rahul Kumar Meena (2020), "Numerical Simulation of Single and Double Slope Solar Still for Different Performance Affecting Variables", *Ijraset*, https://doi.org/10.22214/ijraset.2020.32050

- 75) https://ocw.mit.edu/courses/mechanical-engineering/2-29-numerical-fluid-mechanics-spring-2015/lecture-notes-and-references/MIT2_29S15_Lecture4.pdf
- 76) Lee, H.H., 2021. Finite Element Simulations with ANSYS Workbench 2021: Theory, Applications, Case Studies. SDC publications.